

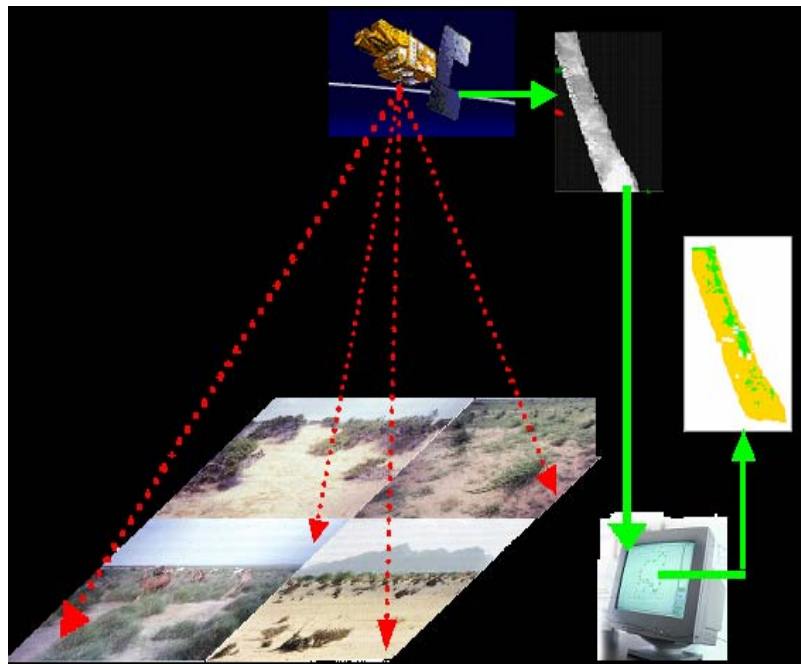
Centre for Geo-Information

Thesis Report GIRS-2004-22

Detecting Habitats of Desert Locust on the Sudan Red Sea Coast Using Satellite Images: *A First Exploration*

Mengistie Kindu Mengesha

April 2004



WAGENINGEN UNIVERSITY

WAGENINGEN UR



Detecting Habitats of Desert Locust on the Sudan Red Sea Coast Using Satellite Images: *A First Exploration*

Mengistie Kindu Mengesha

Registration number 770608-557-030

Supervisors:

Prof. dr.ir.A.K. Bregt
Dr. ir. W. van der Werf
Dr. ir. A. van Huis
Drs. H.M. Bartholomeus

**A thesis submitted in partial fulfillment of the degree of Master of Science at Wageningen
University and Research Centre, The Netherlands.**

April 2004
Wageningen, The Netherlands

**Thesis code number: GRS-80326
Wageningen University and Research Centre
Laboratory of Geo-Information Science and Remote Sensing
Thesis Report: GIRS-2004-22**

To the memories of my parents,

And

To the only one my beloved brother Yihenew Zemenu

Acknowledgements

During the period of my study, I have received various assistance and support from many people and organizations that I am grateful very much. First and for most I am deeply indebted to my supervisors Prof. dr.ir.A.K. Bregt, Dr. ir. W. van der Werf, Drs. H.M. Bartholomeus, and Dr .ir. A. van Huis for kind dedication of their valuable time and endeavor to advice, support and critical reviews throughout my research. Their unreserved professional guidance and supervision helped me to complete this work with its present shape.

I would sincerely like to thank Dr. Gbermedhin Woldwahid, for giving the field data, Dr. Munir Butrous, for providing the GPS setup used during field data collection and Roland van Zoest for providing me digital map of the study area. I wish to extend my gratitude to Dr. Keith Cressman, from FAO, for his useful and quick response for validation of the result of non-surveyed area.

My special thanks goes to Willy ten Haaf, my study advisor, for giving me the complete time and freedom during the course of the study. Especially, facilitating for the extension of my study while I encountered health problems; without your support it would not have been successful at all.

I would like to express my heartfelt thanks to Dr Demel Teketay for his moral, academic, and professional support to peruse my study. I would like to express my gratitude to my employer, the Ethiopian Agricultural Research Organization (EARO), for granting me the study leave. The full cost of my study was covered by the Netherlands Organization for intentional cooperation in higher education (Nuffic) through the University Fellowship Program. I am thankful for this generous financial assistance.

My thanks also will go to all my sincere classmates and friends. Thank for their truly friendship and warmly accompany in this study. I wish you all the best, nothing but the best. It has been an honor and pleasure to have known you.

However, I could not finish without memorizing my parents. Nothing could ever eclipse the true love, the unconditional dedication, and the consistent support they had without knowing the test of education. I could never have achieved my dreams without you. Thank you and I will never forget you in the entire of my life! Last but not least, I wish to express my sincere indebtedness to the only one younger beloved brother Yihenew Zemenu. I thank you for your understanding and patience during this long period of my absence by leaving you to my friends. Abay and Daniel Zellalem, I sincerely appreciate your kindness to look after my little brother.

Above all, I thank the Almighty God for giving me every thing I was wishing but I have nothing to give Him except thanking.

Abstract

Plagues of desert locust are a common threat to agricultural production. In order to prevent plagues, continuous information about desert locust habitats is needed. Ground surveying approach was found to be expensive to cover the vast breeding habitats. This thesis explores possibilities of using satellite images for detecting habitats of desert locust as observed in ground surveys and to check if prediction of such habitats can be made to non-surveyed areas. A typical breeding site (Sudan Red Sea Coast) was selected for the research. On this coast, four plant communities, one of which is a desert locust risk habitat, were identified using ground surveying. Locust habitats were detected using supervised classification methods. The results revealed that MODIS sensor was the best sensor in providing suitable images of the study area for the winter season. With this sensor, it was possible to detect the risk habitats with 77.78% of users accuracy. But this result was dependent on the availability of cloud free images coupled with high cover percentage of the risk habitats. Maximum Likelihood classifier performed better than the three other tested classifiers. A mono temporal classification approach was better than a multi-temporal one. Based on expert knowledge, the predicted result of non-surveyed area (Eritrea) seems to be reasonable. It was concluded that MODIS sensor could detect the habitats of the desert locust on the study area with acceptable accuracy during the winter season. It is recommended that using additional information like soil type of the area increases the accuracy of the result.

Key words: habitats, desert locust, image classifications, satellite images, Red Sea Coast

Table of contents

ACKNOWLEDGEMENTS	IV
ABSTRACT	V
TABLE OF CONTENTS	VI
LIST OF TABLES	VIII
LIST OF FIGURES	IX
ABBREVIATIONS	X
1. INTRODUCTION	1
1.1. BACKGROUND.....	1
1.2. PROBLEM DEFINITION.....	2
1.3. RESEARCH OBJECTIVES	3
1.4. RESEARCH QUESTIONS.....	4
1.5. THESIS OUTLINE	4
2. LITERATURE REVIEW	5
2.1. DESERT LOCUST	5
2.1.1. <i>General characteristics of locust</i>	5
2.1.2. <i>Desert locust habitats and distributions</i>	5
2.1.3. <i>Problems with locust</i>	7
2.1.4. <i>Approaches to control locust</i>	8
2.2. REMOTE SENSING.....	8
2.2.1. <i>Main concept</i>	8
2.2.2. <i>Classifications</i>	10
2.2.3. <i>Multi temporal image classifications</i>	12
2.2.4. <i>Accuracy assessment</i>	12
2.2.5. <i>Applications for mapping of desert locust habitats</i>	14
3. MATERIALS AND METHODS	16
3.1. STUDY AREA.....	16
3.2. DATA	17
3.2.1. <i>Ground truth data</i>	17
3.2.2. <i>Remote sensing data</i>	17
3.3. RESEARCH METHODOLOGY	18
3.3.1. <i>Preprocessing</i>	20
3.3.2. <i>Processing</i>	21
4. RESULTS AND DISCUSSION	24
4.1. SELECTING REMOTE SENSING SENSORS	24
4.2. MONO-TEMPORAL IMAGE.....	24
4.2.1. <i>Classification result of desert locust risk habitats</i>	24
4.2.2. <i>Accuracy assessment of mono-temporal image classifications</i>	25
4.3. MULTI-TEMPORAL IMAGES.....	28
4.3.1. <i>Classification result of desert locust risk habitats</i>	28

4.3.2. Accuracy assessment of multi-temporal image classifications.....	29
4.4. COMPARATIVE ANALYSIS OF MONO TEMPORAL WITH MULTI TEMPORAL RESULTS ..	29
4.5. THE FINAL RISK DESERT LOCUST HABITAT MAP.....	31
4.6. PREDICTION OF NON-SURVEYED DESERT LOCUST RISK HABITATS	32
<i>Validation of the result for non surveyed area</i>	34
4.8. CRITICAL REFLECTION	34
5. CONCLUSIONS AND RECOMMENDATIONS	36
5.1. CONCLUSIONS	36
5.2. RECOMMENDATIONS	37
REFERENCES.....	39
APPENDIXES	42

List of tables

TABLE 1. RISK AND NON RISK HABITATS OF THE DESERT LOCUST ON THE SUDAN RED SEA COAST.	22
TABLE2. EVALUATED SENSORS FOR OBTAINING REMOTE SENSING DATA DURING THE WINTER SEASON OF 2000/2001 ON THE SUDANESE RED SEA COAST.	24
TABLE 3. RANKS OF CLASSIFIERS USING THE CLASSIFIED MONO AND MULTI TEMPORAL IMAGES	30
TABLE 4. COMPARATIVE COVER PERCENTAGE OF THE RISK AND NON-RISK HABITATS OF DESERT LOCUST BY THE MAXIMUM LIKELIHOOD CLASSIFIER USING JANUARY 24, 2001 IMAGE WITH THE COVER % OBTAINED BY GROUND SURVEYING (WOLDIWAHID, 2003).	32

List of figures

FIGURE 1. THE FOUR PLANT COMMUNITIES OF THE SUDAN RED SEA COAST	6
FIGURE: 2. PERCENTAGE OF SAMPLE SITES WITH GREEN VEGETATION IN THE FOUR PLANT COMMUNITY.....	7
FIGURE.3. ELECTROMAGNETIC SPECTRUM	9
FIGURE 4 TYPICAL SPECTRAL REFLECTANCE CURVES FOR VEGETATION, SOIL AND WATER .	9
FIGURE5. LOCATION OF THE STUDY AREA.....	16
FIGURE 6. METHODOLOGY FLOWCHART	19
FIGURE 7 SUMMARY OF ACCURACIES OF EACH CLASSIFIER FOR RISK AND NO RISK HABITATS IN EACH OF THE THREE IMAGES	26
FIGURE 8 SUMMARY OF THE ACCURACIES OF RISK AND NO RISK HABITAT FOR THREE IMAGES OBTAINED BY THE FOUR CLASSIFIERS.....	27
FIGURE 9 USER ACCURACIES OF THE RISK HABITATS FOR THE MULTI-TEMPORAL CLASSIFICATIONS	29
FIGURE 11. FINAL MAP OF THE RISK HABITS OF THE DESERT LOCUST ON THE SUDANESE RED SEA COAST DERIVED BY MODIS IMAGE.....	31
FIGURE 12. DESERT LOCUST HABITAT OF NON SURVEYED AREAS (ERITREA)	33

Abbreviations

ARTEMIS	African Real Time Environmental Monitoring and information System
ASTER	Advanced Space borne Thermal Emission and Reflection Radiometer
DLCC	Desert Locust Control Committee
FAO	Food and Agriculture Organization of the United Nations
GIS	Geographical information systems
GPS	Global Positioning system
GTZ	Gesellschaft fur Techisch Zusammenarbeit
MDM	Minimum Distance to Mean
MHD	Mahalanobis Distance
MIR	Middle Infrared
MLH	Maximum Likelihood
MODIS	Moderate-resolution Imaging Spectroradiometer
NASA	National Aeronautics and space Administration
NIR	Near Infra Red
NOAA	National oceanic and Atmospheric administration
AHHVR	Advanced Very High-Resolution Radiometer
PPL	Parallelepiped
RS	Remote Sensing
SPOT	Satellite Probatoire d'Observation de la Terre
SRSC	Sudan Red Sea Coast
TM	Thematic Mapper (Landsat sensor)

1. Introduction

1.1. Background

Plagues of desert locust, *Schistocerca gregaria* Forsk., have been recognized as a threat to agricultural production in Africa and western Asia for thousands of years (Showler, 1995). Locust scourges are referred to in the different parts of the Christian Bible. For example, Exodus 10: 11-14, Deuteronomy 28:38, 2 Chronicles 6:28.

A single swarm of locust can be small, for example a few hundreds of square meters, or huge, composed of billions of locusts with up to 80 million per square kilometer over an area of more than 1000 square kilometers (Krall, 1995). Plagues often involve hundreds of swarms (Krall, 1995). Desert locusts consume per day approximately an equivalent of their body mass (2 g per day) of green vegetation: leaves, flowers, bark, stems, fruit, and seeds. That is, nearly all crops as well as non-crop plants, are at risk (Showler, 1995). Desert locust damage can be substantial. For instance, in 1954-1955, Morocco lost more than \$50 million (in 1994 dollars) due to desert locusts in six weeks in the Souses Massac Valley alone. In 1958, Ethiopia lost 167,000 tons of grain, which is enough to feed a million people for a year (Steedman, 1988). The Desert locust is thus a common threat to agriculture, subsistence farming and vulnerable pastures, which are indispensable for life to the people withstanding hardship in desert and semi-desert areas of Northern Africa, Middle East and Southwest Asia (Cherlet *et al.*, 2000).

A great number of studies have focused on locust outbreak control (Skaf *et al.*, 1990). Preventive control of localized desert locust outbreaks, defined as sudden increases in populations exhibiting or full fledged gregarious behavior, is the corner stone of the current strategy in containing desert locust (FAO, report on the DLCC, 1999). Efficient early detection and control of these outbreaks ensures not only overall success, but also reduces costs, scale and environmental hazards of chemical control (Cherlet *et al.*, 2000). Early detection and identification of the habitats that serve as a major breeding site of desert locust is crucial. To this end, ground surveying of major breeding sites is recurrently conducted. However, it is difficult to cover the whole locust breeding area using ground surveying (Hielkema, 1977).

At present, it is the concern of many national, regional, and international organizations to ensure continuous monitoring of desert locust in the most effective and efficient manner (Tappan *et al.*, 1991). There is a growing interest in the use of remote sensing technology as source of information regarding to the desert locusts (Voss, 1997). Space systems have unambiguous capability in providing essential information and services used for identification of various habitats. Cherlet *et al* (2000) suggest that satellite based information provides an opportunity for providing real time based, and the necessary synoptic knowledge on the status of habitats potentially favorable for desert locusts.

1.2. Problem definition

Due to the ability of desert locusts to form huge, mobile swarms in their gregarious phase and their feeding on all varieties and parts of plants, their sudden appearance in farmers' fields is a fear-instilling event (Hardweg *et al.*, 2000). Most often locusts do not start at high densities in swarms, but in small low-density populations in suitable pocket habitats (Cherlet *et al.*, 2000). Knowledge of these habitats is useful for early locust detection and control. According to Maxwell-Darling (1936), the Sudanese Red Sea Coast is often an important part of subsequent successful breeding area leading to plagues. Based on detailed ground surveying, the suitable habitats and the density of the desert locusts on the southern part of Sudan Red Sea Coast have been identified during the winter season (Woldewahid, 2003). However, continuous ground surveying is needed to do a basic prevention, control and monitoring of desert locust habitats. Such survey is difficult because extensive breeding occurs mostly in the remote, vast, and rugged Sahara, which precluded timely development of resources to go to critical breeding areas (Showler, 1995a). In addition, inadequate infrastructure and logistics hamper the routine collection of field information in those areas (Cherlet *et al.*, 2000). Therefore, required field surveys are expensive, cover small areas and cannot be frequent.

In view of the various problems in obtaining relevant field information from recession area of the desert locust, at adequate time intervals, forecasters and decision makers recognize remote sensing as a potentially valuable source of information (Hielkema, 1980). To this end, remote sensing images obtained by various sensors have been used to identify the habitats of the desert locust (Hielkema, 1980). The satellite sensor that has primarily been used for habitat studies is the National Oceanic and Atmospheric Administration's (NOAA) Advanced Very High-Resolution

Radiometer (AVHRR) (Wallin *et al.*, 1992). NOAA (AVHRR) data were used in the FAO ARTEMIS system to obtain in frequent synoptic overviews of the vegetation situation over the recession area (Cherlet *et al.*, 2000). However, very sparse vegetation cannot be detected due to low spatial resolution (1km by 1km) of NOAA (AVHRR) images. Others such as Landsat, Satellite Probatoire d'Observation de la Terre (SPOT), Advanced Space borne Thermal Emission and Reflection Radiometer (ASTER), and Moderate-resolution Imaging Spectroradiometer (MODIS) have become new ideal sensors. Compared to NOAA (AVHRR), these sensors have better spatial resolution. They have not been yet tried in the study area for detecting habitats of the desert locust during the winter season.

Habitat mapping using remote sensing images is based on the classification of individual pixels or groups of pixels with similar spectral signatures (Lillesand and Kiefer, 2000). There are four commonly used classification algorithms (classifiers), which are developed to group those pixels into similar classes (habitats). These are Maximum Likelihood Classifier, Minimum distance to Mean Classifier, Mahalanobis Distance Classifier, and Parallelepiped Classifier. These classifiers provide a good classification results based on the nature of the remote sensing data (spectral signature of the habitats) used for the analysis. In addition, the classifiers depend on the type of approaches used, mono-temporal using only one image or multi-temporal using more than one image, during classifications. These classification algorithms together with approaches have not been tried yet in the Sudan Red Sea Coast (SRSC) for detecting habitats of the desert locust using satellite images. Therefore, this study focuses on addressing the mentioned problems to fill the present gaps by linking the ground survey findings of habitats of the desert locust in the SRSC to satellite image of the study area.

1.3. Research objectives

The general objective of this research is to link ground surveying findings of desert locust habitats to its satellite image on the Sudan Red Sea Coast, and to check if prediction of such habitats can be made to non-surveyed areas.

1.4. Research Questions

- Which remote sensing sensor can be used to detect habitats of the desert locust in the Sudan Red Sea Coast during the winter season?
- Can images of the best sensor be used to identify the desert locust habitat with above 70% accuracy?
- Which classification algorithms give the best result of identifying the desert locust habitat?
- Does a multi temporal approach give better accuracy than mono temporal one?
- Is it possible to make predictions of habitats for desert locust in a non-surveyed area?

1.5. Thesis outline

This thesis report is organized as follows:

Chapter 1 Introduces background information, statement of the problem, research objectives, research questions, and the structure of the thesis.

Chapter 2 contains the literature review that focus on describing the general characteristics of the desert locust and their habitat. This chapter also gives the concept of remote sensing and its application for mapping of desert locust habitats.

Chapter 3 describes the study area; the data used and detailed procedure of the developed methodology for this study. This chapter starts with the situation of the study area, and explains characteristics of the data used. Then, the techniques used for the image analysis to drive the habitats of the locust are described.

Chapter 4 presents the outcome of this study. The results are shown and discussed in the order of the methodology to achieve each objective. Tables, figures and maps are used according to the nature of the information.

Chapter 5 presents conclusion of the key findings. Recommendations are also provided in this chapter.

2. Literature review

2.1. Desert locust

2.1.1. General characteristics of locust

The desert locust (*Schistocerca gregaria* Forsk.) is one of a dozen species of short-horned grasshoppers (*Acridoidea*) that are known to change their behavior and form swarms of adults or bands of hoppers (wingless nymphs) (FAO, 1994). It exists in its solitary phase when conditions are not suitable for breeding. A period during which locusts predominantly occurs as solitary phase is called recession (Skaf *et al.*, 1990). When conditions become favorable for breeding, desert locust densities increase which can lead to formation of hopper bands and swarms (Skaf *et al.*, 1990).

2.1.2. Desert locust habitats and distributions

A habitat is a spatial unit that can be occupied by any groups or individual animals or plants independent of the size (Liu, 2001). A habitat provides the necessary combination of ecological components required to support a specific species. That is all habitats include at least a source of food, protective cover and space; and determine the possibility of existence of an individual species (Voss, 1997). Thus, desert locust has specific habitats for breeding (Showler, 1995a). It occurs in desert and scrub regions of northern Africa, the Sahel (region including the countries of Burkina Faso, Chad, Mali, Mauritania, and Niger), the Arabian Peninsula (e.g., Saudi Arabia, Yemen, Oman), and parts of Asia to western India (Steedman, 1988). These regions are characterized by seasonal rainfall averaging between 80 and 400 mm annually, which can vary dramatically from year to year with annual rainfall up to 70% above or below the average (Magor, 1997). Johanson (1926) firstly identified the Red Sea Coastal plains as important breeding areas for desert locust.

The practice of shifting cultivation created many habitats with the Wadies area of the Sudan Red Sea Coast (Steedman, 1988). On this Coast, four important plant communities are found, namely *Suaeda monoica*, *Heliotropium* species, *Panicum turgidum* and *Acacia tortilis*. Only the *Heliotropium* plant community was identified as breeding habitat of the desert locust

2. Literature review

(Woldewahid, 2003). The *S. monoica* plant community is dominated by *S. monoica* and mainly found at the coastal sites (fig 1a). The *Heliotropium* plant community occurs at the transition between the *P. turgidum* grasslands and *S. monoica* shrub, at places where spreading wadies provide for supplemental water. As far as the soils are non salty, the area of the *Heliotropium* plant community is extensively used for cropping millet (*Pennisetum typhoideum* Rich.). This plant community covers only about 5% of the study area but it supported 93-100% of the desert locust (Woldewahid, 2003) (fig. 1b). The *P. turgidum* community is characterised by the preferential species *Panicum turgidum*. *P. turgidum* is a perennial tussock grass that is yellow during summer but produces green sprouts in the rainy season (fig.1c). The *Acacia tortilis* plant community is dominated the widely spread perennial desert shrub *A. tortilis* (fig. 1d).



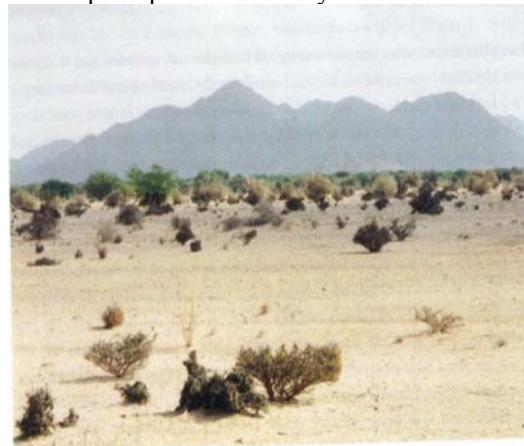
a. Suaeda monoica plant community



b. Heliotropium plant community



c. P. turgidum plant community



d. A. tortilis plant community

Figure 1. The four plant communities of the Sudan Red Sea Coast (Woldewahid, 2003). (a) Suaeda monoica plant community, (b) Heliotropium plant community, (c) P. turgidum plant community, (d) A. tortilis plant community

The greenness of each plant community was shown in Woldwahid (2003). In November 2000, all sites had green vegetation. At the end of January 2001, there were marked differences among plant communities in the greenness of the vegetation, and the greenness of *Heliotropium* plant community much higher than the other plant communities (fig 2).

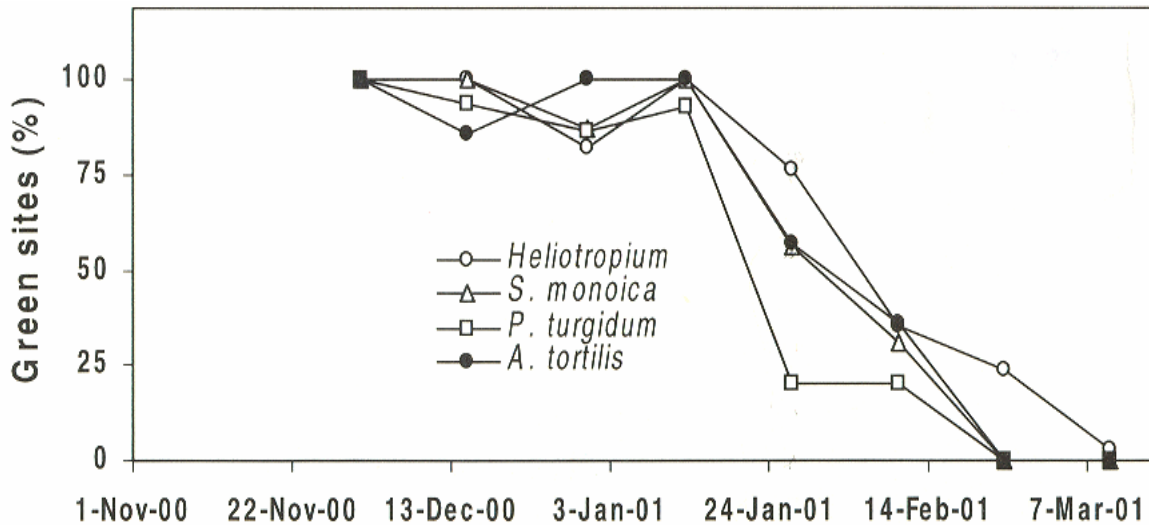


Figure: 2. Percentage of sample sites with green vegetation in the four plant community Woldewahid (2003)

2.1.3. Problems with locust

During the solitary phase, locust populations are low and pose no economic threat. After periods of drought, when vegetation flushes occur in major desert locust breeding areas, rapid population buildups and competition for food occasionally result in a transformation from solitary behavior to gregarious behavior (Showler 1995). Following this transformation, locusts often form dense bands of flightless nymphs and swarms of winged adults that can devastate agricultural areas (Shawler, 1995). An important factor that contributes to the plague status of desert locust is its ability to migrate up to 500 km overnight. Such migrations can only occur if green vegetation has been available during its breeding activity (Skaf *et al*, 1990)

2.1.4. Approaches to control locust

According to Cressman (1996), farmers were responsible to monitor and protect their crop from desert locust invasion. However, they could not manage to protect, and the responsibility shifted to governments and regional organizations. Practically, survey of desert locust consists of three steps: 1) green habitats identification following rainfall; (2) assessments to ensure whether the area is infested; and (3) search for locust infestations to control (FAO, 1994). Nowadays, attention is given to the use of remote sensing technology as a source of information that can make monitoring more effective and efficient.

2.2. Remote Sensing

2.2.1. Main concept

Remote sensing is the science and art of obtaining information about an object, area, or phenomenon through the analysis of data acquired by a device that is not in contact with the object, area, or phenomenon under investigation (Lillesand and Kiefer, 2000).

The energy, which illuminates the target or is emitted by the target itself, is in the form of electromagnetic radiation. A set of electromagnetic radiations of all possible wavelengths is called the electromagnetic spectrum (Lillesand and Kiefer, 2000). It is divided into the following regions: gamma ray, X-ray, ultraviolet, visible, infrared, and radio (Fig.3).

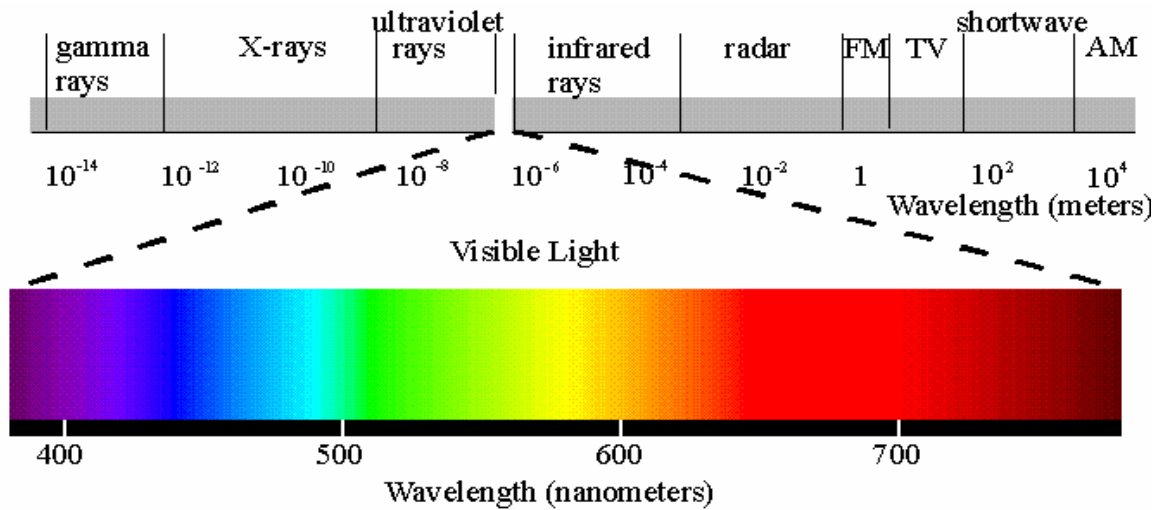


Figure.3. Electromagnetic Spectrum (URL 1)

Remote sensing sensors systems can record information of earth objects from the portions of electromagnetic spectrum. Many earth surface features manifest very distinctive spectral reflectance characteristics that will vary with wavelength. This important property of object allows to separate distinct cover types based on their response values for a given wavelength. When we plot the response characteristics of a certain cover type against wavelength, we define what is termed the *spectral signature* or spectral curve of that cover. Figure 4 illustrates the spectral signatures for some common cover types.

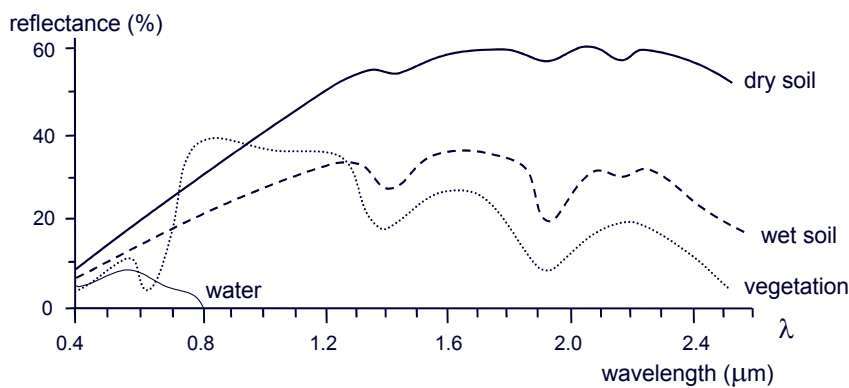


Figure 4 Typical spectral reflectance curves for vegetation, soil and water (Lillesand and Kiefer, 2000).

The satellite sensor that has primarily been used for habitat studies is the NOAA (AVHRR) (Wallin *et al.*, 1992). This sensor has nearly a daily repeat cycle and a 1-km spatial resolution. Both the temporal density of the data and the moderate spatial resolution make this sensor well suited for studying large area habitat. Other moderate resolution satellite sensors include SPOT vegetation (1 km data, launched in 1998), ASTER (15 m data, launched in 1999), Landsat (30 m data, launched in 1972) and MODIS (250 m, 500 m, and 1 km data, launched in 1999). These sensors have the proper instrumentation for habitat studies. Each of these sensors has improved geometry, radiometry, and calibration compared to the AVHRR (Davis *et al.*, 2002).

2.2.2. Classifications

Classification is producing meaningful information via identification of individual pixels or groups of pixels with similar spectral responses (spectral signatures) to incoming radiation (Zhan, 2003). Ideally, pixels are expected to be more or less grouped in the multispectral space in clusters corresponding to different land cover types (Keuchel *et al.*, 2003). If classes do not have distinct clusters in the feature space, image classification can only give results to a certain level of reliability (Janssen, 2001). There are two general types of classifications: unsupervised and supervised. In both cases, previous knowledge of the imaged scene is highly desirable (Jensen, 1996). Unsupervised classification compares pixel spectral signatures to the signatures of computer determined clusters and assigns each pixel to one of these clusters. In supervised classification, the image analyst supervises the pixel categorization process by specifying, to the computer algorithm, numerical descriptors of the various land cover types that exist in an image. Training samples that describe the typical spectral pattern of the land-cover classes are defined. Pixels in the image are compared numerically to the training samples and are labeled to the land-cover class that has similar characteristics. Supervised classifications require up-front knowledge of the scene area in order to provide the computer with unique material groups or what are called "training classes". The resulting classification maps should be checked using ground truth information and field validation surveys if possible. In general, supervised classifications are more accurate than unsupervised (Jensen, 1996). There are four commonly applied classification algorithms to group the objects/classes in to similar classes. These include Maximum Likelihood Classifier, Minimum distance to Mean Classifier, Mahalanobis Distance Classifier, and Parallelepiped Classifier. These algorithms are described in details.

Maximum Likelihood (MLH) Classifier. This Classifier quantitatively evaluates both the variance and the covariance of the trained spectral response patterns when deciding the fate of unknown pixel. It is based on a normalized (Gaussian) estimate of the probability density function of each class (Pedroni, 2003). It assumes that the distributions of the points for each cover-type are normally distributed and under this assumption, the distribution of a category response can be completely described by the mean vector and the covariance matrix. Given these values, the classifier computes the probability that unknown pixels will belong to a particular category. The principal drawback of MLH classifier is large number of computations required to classify each pixel (Lillesand and Kiefer, 2000). This is particularly true when either a large number of spectral channels are involved or a large number of spectral classes must be differentiated. In such cases, maximum likelihood classifier is much slower computationally than the other techniques (Lillesand and Kiefer, 2000).

Minimum Distance to Mean (MDM) Classifier. Calculates the mean spectral value in each band and for each category, relates each mean value by a vector function, and after computing the distance; the unknown pixel is assigned to closest class. A pixel of unknown identity is calculated by computing the distance between the values of unknown pixel and each of the category means. It is mathematically simple and computationally efficient, but it has certain limitations. Most importantly, it is insensitive to different variance in the spectral response data. Because of such problems, this classifier is not widely used in applications where spectral classes are close to one another in the measurement space and have high variance (Lillesand and Kiefer, 2000).

Mahalanobis Distance (MHD) Classifier. It is similar to minimum distance, except that the covariance matrix is used in the equation. Variance and covariance are figured in so that the clusters that are highly varied lead to similarly varied classes, and vice versa. From all clusters, k points per cluster are selected nearest to the point to be assigned. This new point is assigned to the cluster for which the average distance of k points to this new point is minimum.

Parallelepiped (PPL) Classifier. It is sensitive to variance by considering the range of spectral values in each categories training sets (Lillesand and Kiefer, 2000). This range is defined by the highest and lowest digital number value in each band and appears as a rectangular area. An unknown pixel is classified according to the category range, or decision region, in which it lies or as “unknown” if it lies outside all regions. Parallelepiped classifier is very fast and efficient

computationally (Lillesand and Kiefer, 2000). PPL classifier encounters difficulties when decision regions overlap (Lillesand and Kiefer, 2000). Pixels lie in the overlapping areas are classified as “not sure” or just arbitrarily as one or both of the overlapping classes.

2.2.3. Multi temporal image classifications

A mono-temporal image analysis, which relies on one image obtained at a single point in time, is usually used for classification of different vegetation types (Wagner *et al.*, 1993). However, sometimes it does not work well for classification of vegetation species types which have similar spectral signatures (PaxLenney *et al.*, 1997). To solve such problem, different studies are going on to explore the possibility of using a multi-temporal classification approach so that to identify the differences of the vegetation types exhibiting on the various temporal stages (Wagner *et al.*, 1993). Rogan *et al.* (2001) found that multi-temporal images provide significant improvements in accuracy of vegetation classifications.

2.2.4. Accuracy assessment

Accuracy assessments determine the quality of the information derived from remotely sensed data (Padroni, 2003). No classification is complete until its accuracy has been assessed (Lillesand and Kiefer, 2000). In this context, “accuracy” means the level of agreement between labels assigned by the classifier and the class allocations on the ground collected by the user as test data. When performing accuracy assessment for the whole classified image, the known reference data should be another set of data, different from the set that is used for training the classifier. One means of expressing classification accuracy is the preparation of an error matrix (Appendix A). The Error matrix compares the relationships between known reference data (ground truth) and the corresponding result of classifications. With the error matrix, several accuracy indices such as overall accuracy, user’s accuracy and producer’s accuracy can be assessed. The detailed descriptions of these three accuracy indexes are explained below according to Lillesand and Kiefer (2000). The formulas are obtained from the matrix showed in Appendix A.

Overall accuracy is the proportion of all reference pixels that are classified correctly (in the sense that the class assignment of the classification and of the reference classification agree). It is computed by dividing the total number of correctly classified pixels (the sum of the elements

along the main diagonal) by the total number of reference pixels (formula 1). It gives no information about what classes are classified with good accuracy.

$$\text{Overall accuracy} = \frac{\sum_{k=1}^N a_{kk}}{\sum_{i,k=1}^N a_{ik}} = \frac{1}{n} \sum_{k=1}^N a_{kk} \quad \text{-----} 1$$

Where:

$$\sum_{k=1}^N a_{kk} = \text{total number of correctly classified pixels (the sum of the elements along the main diagonal) (Appendix A)}$$

$$\sum_{i,k=1}^N a_{ik} = \text{total number of reference pixels}$$

N = number of classes

Producer's accuracy is computed by dividing the number of correctly classified pixels in each category (on major diagonal) by the number of training set pixel used for that category (the column total) (formula 2). This figure indicates us how well the training pixel of the given cover type are classified

$$\text{Producers accuracy (class I)} = \frac{a_{ii}}{\sum_{i=1}^N a_{ki}} \quad \text{-----} 2$$

Where:

a_{ii} = number of correctly classified pixels in each category (on major diagonal)

$$\sum_{i=1}^N a_{ki} = \text{the number of training set pixel used for that category (the column total)}$$

User's accuracy is computed by dividing the number of correctly classified pixels in each category by the total number of pixels that is classified in that category (the row total) (formula 3). This figure indicates the probability that a pixel classified in to a given category actually represents that category on the ground.

$$\text{Users accuracy (class I)} = \frac{a_{ii}}{\sum_{i=1}^N a_{ik}} \text{-----3}$$

Where:

a_{ii} = number of correctly classified pixels in each category (on major diagonal)

$\sum_{i=1}^N a_{ik}$ = the total number of pixels that is classified in that category (the row total)

2.2.5. Applications for mapping of desert locust habitats

Spurred on by the desert locust plague of 1988, there have been urgent and repeated request of international bodies such us Food and Agriculture Organization of the United nations (FAO), the European Community and the African Development Bank for remote sensing techniques to be applied and installed (Tucker et al., 1995). Recent improvements in satellite image availability have made it possible to perform image analysis at much larger scale than in the past. This leads a much wider use of satellite images as a source of timely available spatial data (Pax-Lenney, *et al* 2001). Remote sensing technologies have also greatly increased the capabilities of mapping various habitats. The FAO groups pointed out that Satellite data provides information for detection areas where vegetation conditions are suitable for desert locust breeding and development (FAO, 1994). Especially, improved remote sensing information can assist in timely pinpointing those areas where the potential for significant breeding and the danger of desert locust upsurges exist.

A result obtained during the study on the use of remote sensing techniques for desert locust survey and control (march-June 1976) in Africa, justified a more detailed investigation on the

potential use of remote sensing data derived from Landsat. The result showed that Landsat satellites are promising for the detection of small area of both ephemeral and perennial vegetations under desert conditions. However, due to lack of sufficient field data and materials, the result was not conclusive to define the potentials of Landsat system for cost effective monitoring in operational context (Hielkema, 1980).

In 1990 GTZ (Gesellschaft für Technische Zusammenarbeit, Germany) started the pilot project “Integrated Biological Control of Grasshopper and Locust”. One part of the project has concentrated on the mapping of the potential desert locust breeding habitats using remote sensing techniques. GTZ project was started with the Tokar Delta, a recession area on the Sudan Red Sea coast and images from Landsat Thematic Mapper(TM) were used for mapping the desert locust habitats. They found the possibility of mapping the desert locust habitat using these images (Voss *et al.*, 1997).

In general, the currently available satellites cannot directly detect individual locusts or locust swarms. Some highly sophisticated satellites used by the military and forthcoming civilian satellites could potentially locust swarms but these images are not yet available (URL 2).

3. Materials and Methods

3.1. Study Area

The study area was the Red Sea Coastal plain of Eastern Sudan between Port Sudan and Tokar. The geographical boundaries are 19°35'N, 37°13' E in the North, and 18°26'N, 37°44'E in the South, the Red Sea in the East and the Red Sea hill in the West (fig 5). This coastal plain is 20 to 40 km wide. The warmest month of the year in the coastal plain is August and the coldest month is January. Precipitation occurs in the winter months from October to January, which is the most favorable period for breeding of desert locust (Woldwahid, 2003).

The soil in the study area mainly consists of coarse and fine sand. The coastal plain has four plant communities, which are mentioned in detail in the literature review under section 2.1.2.

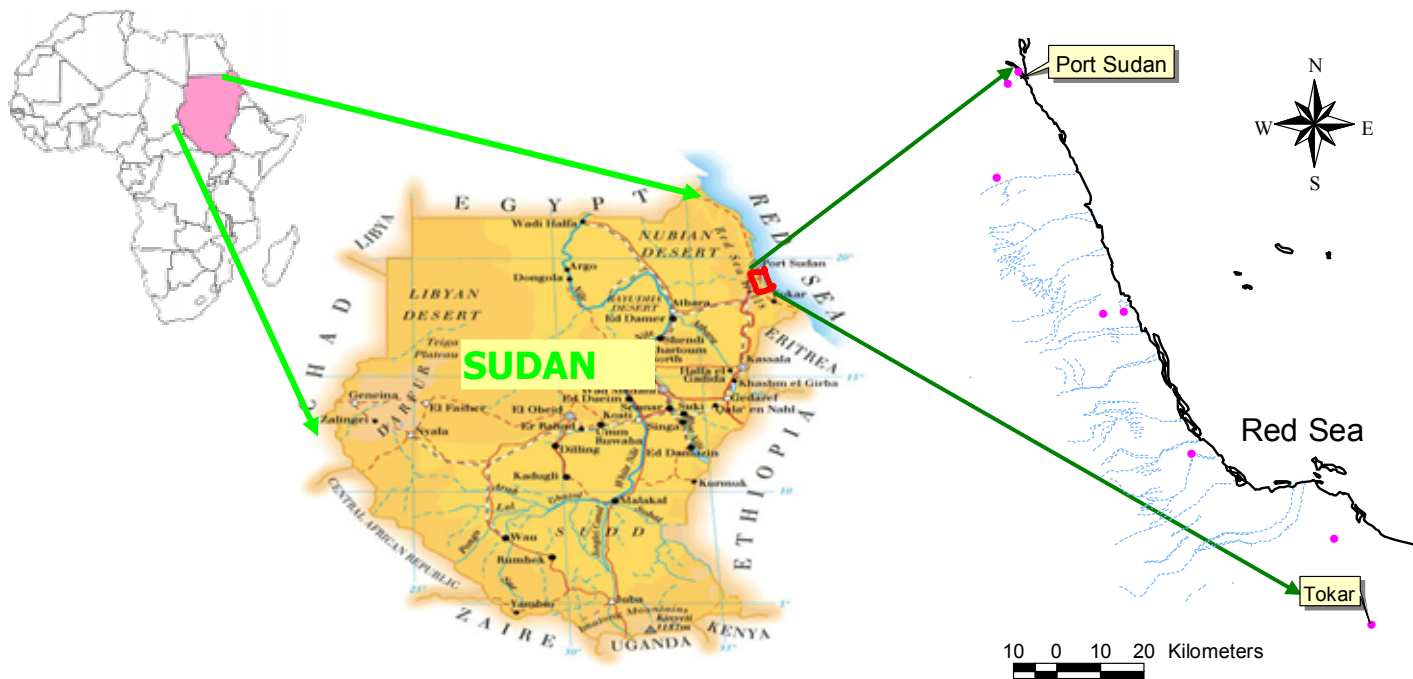


Figure5. Location of the study area

3.2. Data

3.2.1. Ground truth data

The field data used for this study was collected by a collaborative team of Wageningen University, the FAO and the Plant Protection Directorate of Sudan. During the winters of 1999-2000, 2000-2001 and 2001-2002, the team carried out intensive sampling (>100 sampling points) to map plant communities and associated locust populations in the above-delineated area of approximately 20×120 km using a 5×5 km grid (Woldewahid, 2003).

Based on the availability of the remote sensing images and the situation of the study area, the field data of 2000/2001 was chosen for this study. During the year 2000/2001, the cover abundance of all plant species was determined at 64 sample sites. Co-ordinates were determined using a Garmin 12XL GPS at the beginning of each transect and directions taken by compass. Cover abundance was estimated in three 10×10 m plots, located at 50, 200 and 350 m along a 400 m transect. At each sample site, transects and plots were selected to represent relatively homogeneous vegetation. Cover abundance scores in the three plots per transect were averaged to use it for data analysis. The detail of the field data collection can be obtained in the report of Woldwahid (2003).

3.2.2. Remote sensing data

To acquire the remote sensing data for this study; Landsat, ASTER, SPOT, and MODIS sensors were checked. Landsat 7 was launched on April 15, 1999. It has a new Enhanced Thematic mapper plus (ETM+) with 7 spectral bands and with 15 m spatial resolutions. It has a capability of viewing every 16 days (URL, 3). ASTER was launched on December 18, 1999. It has also a capability of taking image every 16 days with spatial resolution of 15 m to 90 m. The SPOT 5 satellite sensor was launched on May 3, 2002, which has capability of taking images every 10 days with spatial resolution of 20 m (URL, 4). MODIS was launched on December 18, 1999 and began collecting data on February 24, 2000. It has capability of viewing the entire Earth's surface every 1 to 2 days, acquiring data in 36 spectral bands, or groups of wavelengths between 0.4 and 14.5 μm , with spatial resolutions of 250 m (bands 1-2), 500 m (bands 3-7), 1000 m (bands 8-36) (see

Appendix B for MODIS Technical Specifications). MODIS has different available products, which are free and easy to download from Internet. MODIS has better spatial and spectral resolution than the NOAA sensor, which can allow for more accurate and large-scale change detection of vegetation conditions. Moreover, it has more temporal availability of data than the Landsat sensor.

In this study, a 250-meter (band 1 and 2 or Red and Near infrared) surface reflectance with Sinusoidal projection of MODIS surface reflectance product (MOD09GQK) was used. The product is an estimate of the surface spectral reflectance for each band to produce a measurement equivalent to a ground-level measurement with no atmospheric scattering or absorption (URL 5).

MODIS images that cover the study area were taken in same year and season of ground data to extract satellite information of the plant community.

3.3. Research methodology

The appropriate sensor for this study was selected. Three suitable images were acquired. Both the ground data and the remote sensing data (images) were prepared. For the mono temporal approach, supervised classifications were performed using each of the prepared images. After classifying, the accuracies of the results were assessed by means of error matrix. For the multi-temporal, images were stacked with different combinations and classified following the same procedure as mono temporal approach. The classified results from the mono temporal and multi-temporal approaches were compared. This resulted in final desert locust risk habitat of surveyed area. Predictions of risk desert locust habitat were done by extrapolating spectral signature of the surveyed area to non-surveyed area. Expert knowledge based approaches were used for validation of the prediction result. The overall procedure is illustrated in figure 6.

3. Materials and methods

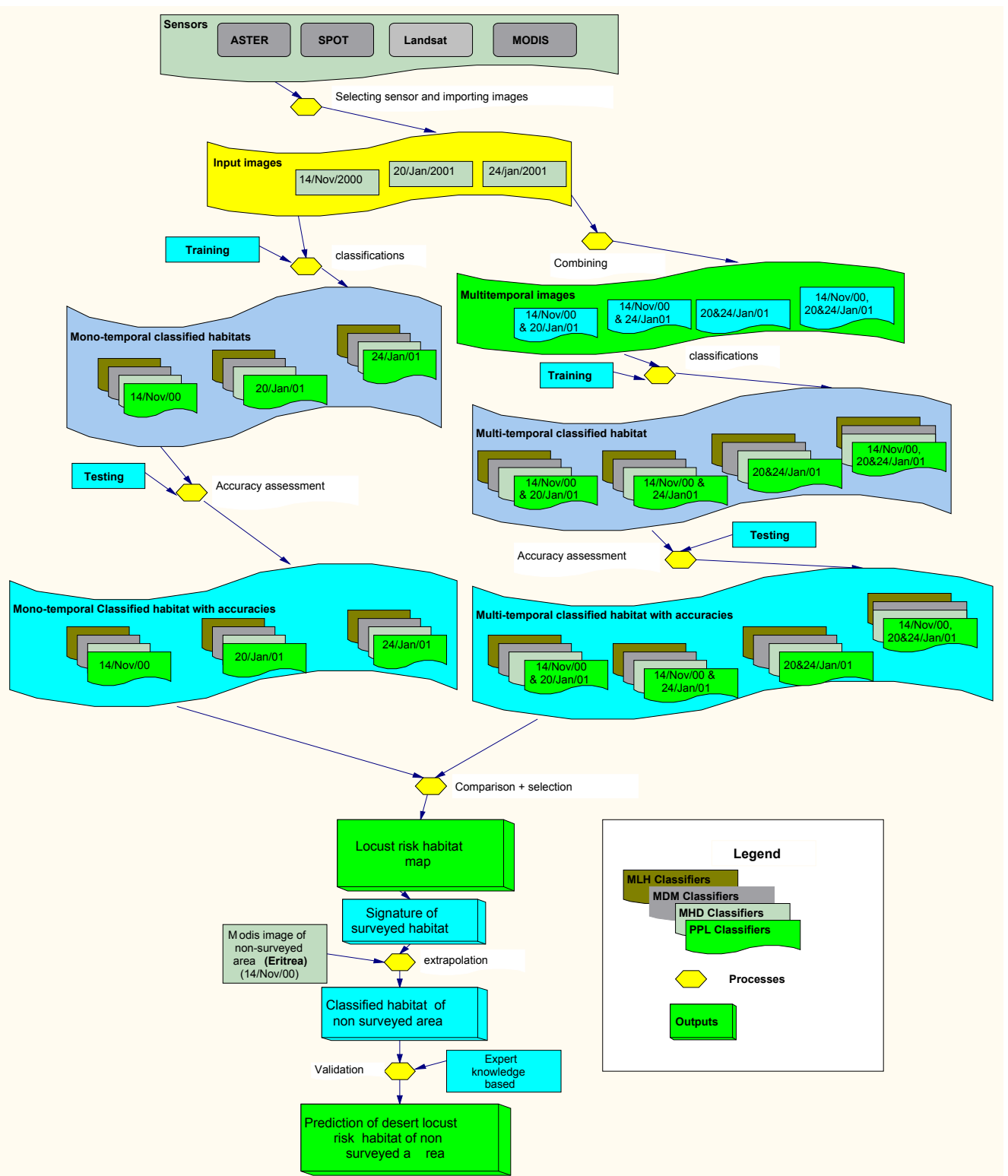


Figure 6. Methodology flowchart

3.3.1. Preprocessing

a. Training and Test Sets preparation

Sixty-four vegetation samples that were collected in the winter season of 2000/2001 were used for this study. The sample sites were divided into two sets. The first set, which has 23 of the total samples, was used for the training sites during classification of the locust risk habitat for both mono and multi-temporal image of the study area. The remaining 41 sample sites were not enough to use as testing sites. Testing sites should be enough to be representative for accuracy assessments (Lillesand and Kiefer, 2000). Therefore, one additional sample site to each of the testing sample sites was collected from the image by using the coordinates and the directions taken during field data collection. As a result, a total of 82 testing sites were used and labeled as second set.

b. Selecting Remote Sensing Sensors

The availabilities of suitable images were checked from different remote sensing sensors during the winter season of 1999/2000, 2000/2001 and 2001/2002 (URL 3, 4 & 5). The visited sensors for the purposes of this study were Landsat, ASTER, SPOT, and MODIS sensors. Based on the availability and image quality (cloud cover), the best sensor was selected for this study.

c. MODIS image Acquisition and Importing

The free MODIS products were collected from the website of the EOS data gateway (URL 2). After checking the overall quality, more than 100 images of the MOD09GQK product from November 2000 to March 2001 were selected and downloaded. These products are provided by the EOS gateway in HDF format, and they are not readable to the software ERDAS Imagine 8.5 which is used for this study. Therefore, all of the downloaded data were converted into IMG format using import function of the ERDAS Imagine 8.5.

d. Quality Control and Sub Setting to Study Area

MODIS provides quality control information that allows to screen each pixel and to determine whether it is appropriate for scientific analysis (URL 5). Quality Control Data of the MOD09GQK products is given by band 3 with cell value of 4096. Using Modeler function of ERDAS Imagine 8.5, cells in band 1&2 were filtered and remained only if their values in band 3 were equal to 4096.

The study area covered only small part of the MODIS image. Therefore, after quality control, the image is subsetting to the study area. These operations were carried out on each of the three downloaded MOD09GQK products.

3.3.2. Processing

a. Training Computer and Signature Evaluation

The prepared training samples were used for training the computer and signatures of these samples were collected. Before performing classifications, the signatures of these training sites were studied in order to get an accurate idea about the position and the size of the classes in the feature space. In addition, signature evaluation was used to see if signatures of different objects were well separated, or if were overlapping in the feature space plot, which help to decide to merge the signatures or not.

b. Image Classifications

Supervised classifications were performed using image signature collected by training site (section 2.2.3). The classifications were done per plant community level. Then, the classified plant communities were merged to generate a total of two classes, which are a risk and non- risk desert locust habitats. Desert locust risk habitats in the context of this research are those plant communities, which can support 93-100% of desert locust (Table 1). This habitat covers 5% of the study area (Woldwahid, 2003).

3. Materials and methods

Table 1. Risk and non risk habitats of the desert locust on the Sudan Red Sea Coast.

Classes	Plant communities	Area (%)	Desert locust density (%)
Risk	Heliotropium	5	93-100
No risk	S. monica, P. turgidum, A. tortilis	95	-

Four classification algorithms; MLH Classifier, MDM Classifier, MHD Classifier, and PPL Classifier were tested over the three images to select the best one.

For the multi-temporal analysis, combination of images were stacked using ERDAS imagine function. Firstly, image of November 14, 2000 with January 20, 2001 was stacked. Secondly, Image of November 14, 2000 with January 24, 2001; and thirdly, January 20, with that of January 24, 2001 was stacked. Finally, the combinations of the three mono temporal images were stacked. Each of the stacked images was classified using the above-mentioned classifiers.

c. Accuracy Assessment

Accuracies of both mono-temporal and multi-temporal classification results of the risk and no risk habitats were assessed using separate testing sites and presented in the form of error matrix. Error matrix compares the relationships between known reference data (ground truth) and the corresponding classification results (Lillesand and Kiefer, 2000). It is shown in the form of overall accuracy, users accuracy (the probability that a classified “risk” habitats is a true “risk” habitat), and producer’s accuracy (the probability that a “risk” habitat will be classified as risk habitats).

d. Predictions of Habitat to Non surveyed Area

MODIS image was used for predicting the habitats of the desert locust on non-surveyed area. It was checked in Eritrea between Shirumkelib (17⁰42’N/38⁰23’E) and Akbanazouf Plains (15⁰57’N/39⁰12’E). This area is a focal point of FAO for forecasting desert locust (URL 6).

The spectral signatures of surveyed area tested by the best classifier were chosen for predicting the habitats on non-surveyed area. These signatures were extrapolated to the non-surveyed area

3. Materials and methods

using ERDAS imagine. The best classifier obtained on non-surveyed area was used and supervised classifications were performed. The predicted results were validated using expert knowledge.

4. Results and discussion

4.1. Selecting Remote Sensing Sensors

Out of the four visited sensors (Landsat, ASTER, SPOT, and MODIS), MODIS sensor is the only one that provides images during the winter season on the Sudan Red Sea Coast (Table 2). Winter season of the SRC is a period favorable for the growth of plant community, which creates suitable conditions for the breeding of desert locust. The field data was taken during such season, which is often cloudy. Using the other three sensors, the maximum amount of images available is limited to about 1 or 2 per month because of the low revisiting time (URL 3). Therefore, the probability to get only cloudy images is very high.

When image are ordered or assessed the image producer indicate the cloud percentage per scene (the whole image viewed at a time). The study area only covered small part of the scene. Even if 100 images which are considered cloud free, were obtained from the image producer, only three images were suitable to use for the study area (Table 2). The clouds cover in the study area, which are very near to the Red Sea Coast, made other images useless for this analysis.

Table2. Evaluated sensors for obtaining remote sensing data during the winter season of 2000/2001 on the Sudanese Red Sea Coast.

Sensors	Return images per month	Image without clouds	
		Indicated by producer (scene)	Actual case (in the study area)
Landsat	1 to 2	-	-
ASTER	1 to 2	-	-
SPOT	2 to 3	-	-
MODIS	Every day	100	3

4.2. Mono-temporal image

4.2.1. Classification result of desert locust risk habitats

Two classes, risk and no risk habitat were obtained. Different classifiers were tested using three images acquired in the winter season of year 2000/2001. These three images were classified individually with four classifiers. Each of these classifiers resulted in the possibility of

discriminating the risk locust habitat from no risk habitats (Appendix C). To check the performance of each classifier accuracy assessments were done.

4.2.2. Accuracy assessment of mono-temporal image classifications

The accuracy of mono-temporally classified images of 14 November 2000, 20 January 2001, and 24 January 2001 were assessed.

Figure 7 shows the summarized accuracies of each classifier using the three-classified mono temporal images. In this figure, it was found that the performance of each classifier in each of these three mono-temporal images in detecting both risk and non-risk desert locust habitats by using the three accuracy indexes (producers, users and overall accuracies). These figures are obtained based on the error matrix shown in Appendix D.

In the image of November 14, 2000, Maximum likelihood classifier resulted better accuracy than other classifiers. (Fig 7a). Minimum distance to Mean Classifier showed best classification accuracies than other classifiers using January 20, 2001 image (fig 7b). In addition, this image has better accuracy than that of the November 14, 2000. The classifications accuracy result obtained by January 24, 2000 image was the best of the three images (fig 7c).

4. Results and discussion

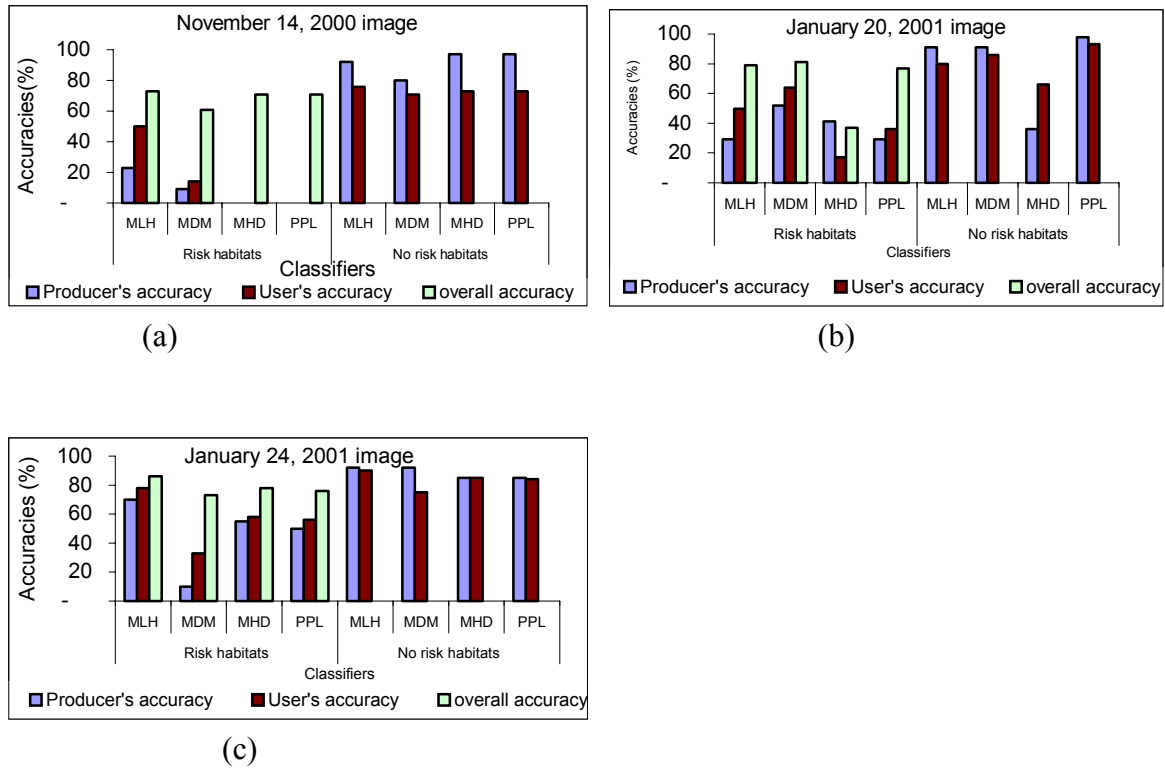


Figure 7 Summary of accuracies of each classifier for risk and no risk habitats in each of the three images. (a) November 14, 2001; (b) January 20, 2001; and (c) January 24, 2001 images. (MLH: Maximum Likelihood Classifier, MDM: Minimum distance to Mean Classifier, MHD: Mahalanobis Distance Classifier, and PPL: Parallelepiped Classifier)

Careful inspection was given for the risk habitats since it is the major focus of this study to pinpoint these risk habitats of the desert locust. Overall accuracies of the classified risk habitats were much higher than the other two accuracy indexes (users and producers) in each of the three images. For instance, Mahalanobis Distance Classifier resulted in 70.73 % overall classification accuracy using November 14, 200011 images and null for the producers and users accuracies of the risk habitats. The reason for such big overall accuracy is result of the approach used for grouping the four plant community into two classes (risk and no risk habitats) (section 3.3.2). Calculation of the accuracies using error matrix, were based on the two classified risk and no risk habitats. Grouping of the three plant communities as no risk habitats for the calculation may over or underestimate the accuracies. Overall accuracy is measured by using the total correctly classified habitats divided by reference (testing habitats) (section 2.2.4). Therefore, these

4. Results and discussion

problems resulted in high overall accuracies of the classified risk habitats and a decision was made to skip it, as it did not achieve the main goal of this particular study.

Careful inspection was given for the risk class since it is the major focus of this study to pinpoint these risk habitats of the desert locust. Special attention was also given to the user's accuracy. Using the user's accuracy, it is possible to know the probability that a classified "risk" habitat is a true "risk" habitat. With this, the summarized user accuracies of the risk habitat for the mono temporal images are shown in figure 8. The result showed that risk habitats were discriminated with user's accuracy of 77.78% by using MLH classifier.

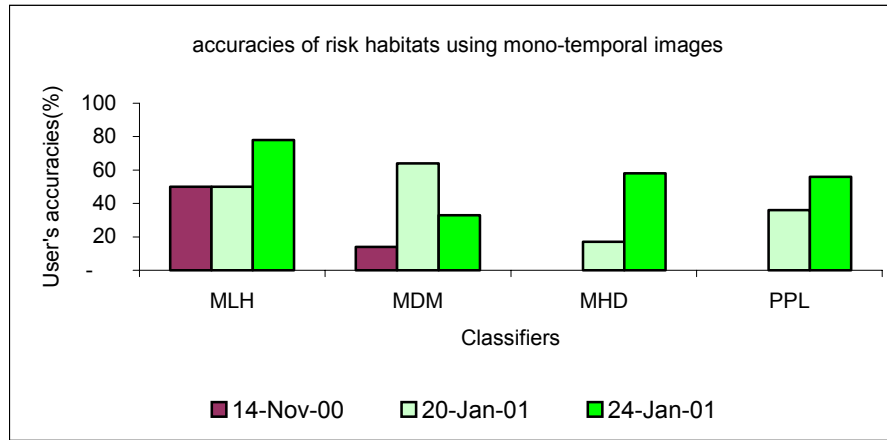


Figure 8 Summary of the accuracies of risk and no risk habitat for three images obtained by the four classifiers.

The accuracy assessment results of the mono temporal classification showed that Maximum likelihood classifier performed better than the other three classifiers in each of the three images except the January 20, 2001. To identify the cause of such problem in January 20, 2001 image, it was checked whether the image fulfilled the required assumption of MLH classifiers or not. It was found that the data were normally (Gaussian) distributed (Appendix G -fig1). The problem was due to overlap of the classes (the plant communities) in the feature space plot (Appendix G-fig 2). The pixel values of the two bands were plotted in a two-dimensional diagram as vectors, this forms the feature space plots of the image. In the feature space, it was expected that each plant community would accumulate to distinct clusters by having distinct spectral pattern. The southern parts of this image were too cloudy and were not used for the analysis. Pixels with risk

habitat information might be lost and showed too much overlap of the four plant communities toward the soil line. MLH classifier computes the probability that unknown pixels will belong to a particular category and in case of much overlapping results in poor separable classes (habitats (URL, 7). In such cases, the Minimum distance to mean show better as it considers computing the distance between the values of unknown pixel and each of the categories means during deciding the fate of unknown pixels.

The MHD and PPL classifiers showed low accuracy result (no users accuracy of risk habitats) in the November14, 2000 image. The MHD and PPL classifiers have problems if the clusters of pixels are not highly varied (similar) and when pixels are quite far from the mean respectively (section 2.2.2). It could be such reason resulted in low accuracy.

The user accuracy of the classified risk habitats using 24 January 2001 image was by far better than the two others (fig 8). Woldewahid (2003) showed that in November 2000, all the sites had green vegetation. At the end of January 2001, there were marked differences among the plant communities, and the greenness of *Heliotropium* plant community (risk habitat) was much higher than the other plant community. This could be one of the reasons of variations in accuracies between these images. However, major differences of accuracies were observed between classification made based on the 20 and 24 January 2001, which in reality do not have been expected that much. This big leap of accuracy may be loss of information due to the presence of clouds in the southern part of the study area (Appendix C-fig 2).

4.3. Multi-temporal images

4.3.1. Classification result of desert locust risk habitats

The images were combined and resulted in four different combined images. Each image was classified using the four classifiers. The results showed that risk habitats are distributed throughout the study area (Appendix E). The accuracies of the classified results were calculated.

4.3.2. Accuracy assessment of multi-temporal image classifications

The accuracies of multi-temporal classified images, which were combined 14 November 2000 with 20 January 2001; 14 November 2000 with and 24 January 2001; 20 January 2001 with 24 January 2001 and the combination of the three images were assessed in order to find the best classifier. Attention was given to user's accuracy of the risk habits. Figure 9 shows that user's accuracy of each classifier using the multi-temporal images with different combinations. The largest users accuracy obtained was 50 % and the lowest was 15 %. These figures are obtained based on the error matrix shown in Appendix F. The combined multi-temporal image of 14 November 2000 with 24 January 2001 showed better accuracy than 14 November 2000 with 20 January 2001. MLH classifier showed better users accuracy than the rest.

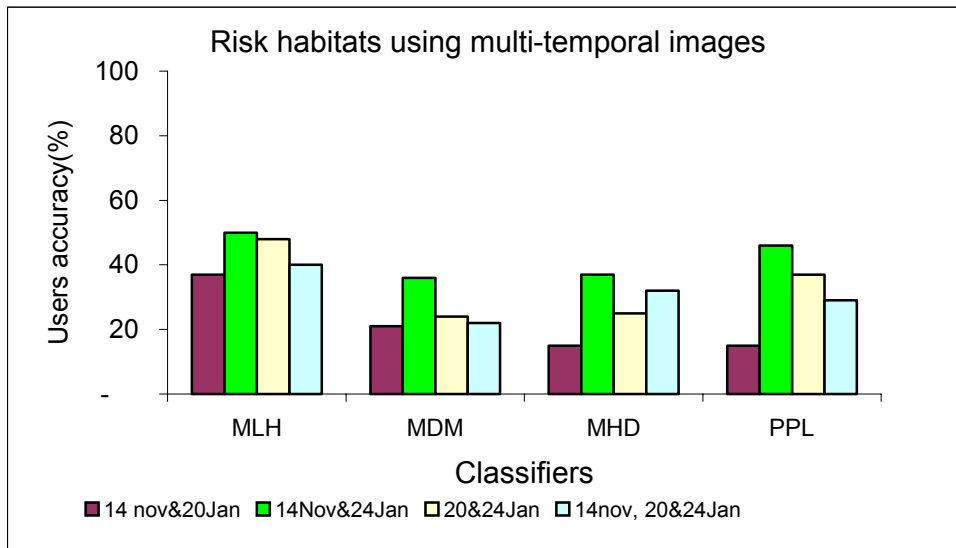


Figure 9 User accuracies of the risk habitats for the multi-temporal classifications

4.4. Comparative analysis of mono temporal with multi temporal results

Comparative analyses of mono temporal with multi-temporal classified result of each classifier were done, by using ranking method. The performances of each classifier in each mono temporal and multi-temporal classified image were ranked based on the user accuracies of the risk habitat.

4. Results and discussion

Value 1 was given for the best classifier and 4 the least. MLH classifiers scored value 1 in all conditions except in image of January 20, 2001(table 3).

Table 3. Ranks of classifiers using the classified mono and multi temporal images

Classifiers	Mono temporal images			Multi temporal images			
	14-Nov	20-Jan	24-Jan	Nov 14 & Jan20	Nov 14 & Jan24	Jan 20 & 24	Nov14, Jan 20 & 24
MLH	1	2	1	1	1	1	1
MDM	2	1	4	2	4	4	4
MHD	3	3	2	3	3	3	2
PPL	3	4	3	4	2	2	3

The user's accuracies of the classified risk habitat obtained by mono-temporal approach showed better result than the multi-temporal approach (fig 10). These results are contrary to Rogan *et al.* (2001) findings that multi-temporal images provide significant improvements in accuracy of vegetation classifications. The reason of low accuracy could be the data set used for the analysis. Only one of the three images showed good classification result. The reasons why the two images taken in November 14, 2000 and January 20, 2001, resulted lower classification accuracies are explained in section 4.2.2. There was no other option to get a suitable additional MODIS images during the winter season of the study area for the multi-temporal analysis. Therefore, different combinations of these available images were used for the analysis. Combing good data with poor data reduced the classification accuracy. This has been observed in the multi-temporal classified images using combined image of November 14, 2000 and January 24, 2001 images and their individual classification result.

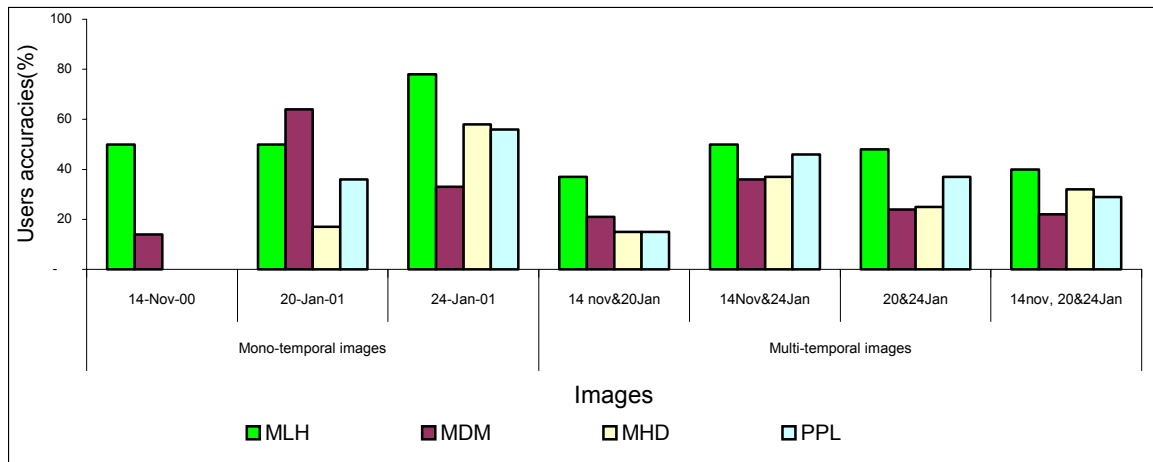


Figure 10. Users accuracy summary of classified risk habitats by mono-temporal with multi-temporal images

4.5. The final risk desert locust habitat map

The Maximum likelihood classifier, which is the best classifier found in this study and image of January 24, 2001 were used to develop the final map of the risk habitats. The result showed that the risk habitats are following the Red Sea Coastal Plain at the Wadies out flows (fig. 11).

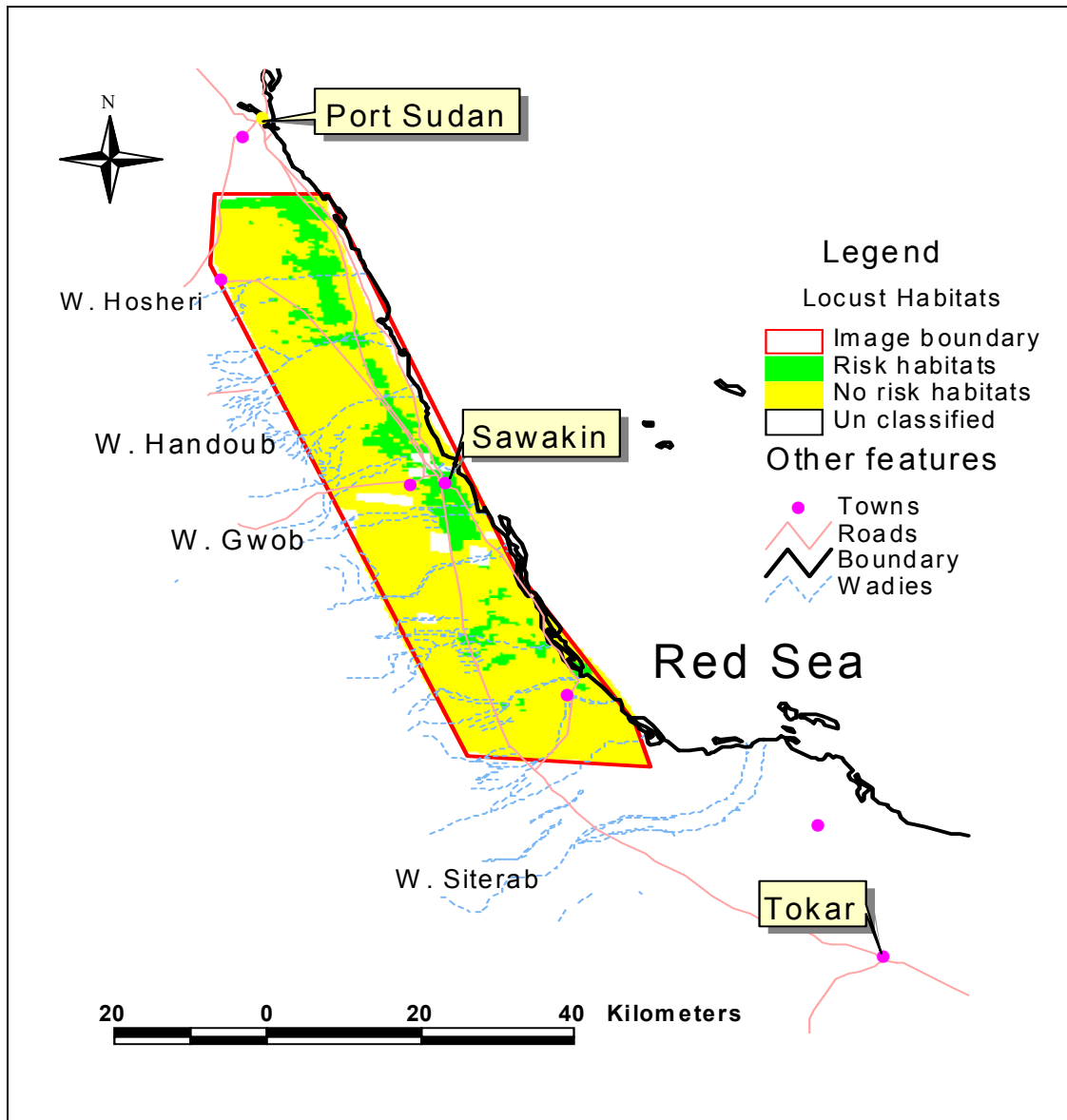


Figure 11. Final map of the risk habits of the desert locust on the Sudanese Red Sea Coast derived by MODIS image (January 24, 2001) using maximum likelihood classifier. Risk habitat indicates *Heliotropium* plant community. No Risk habitat includes *Panicum turgidum*, *Suaeda monoica*, and *Acacia tortilis* plant communities. Roads, Wadies and towns were included for better interpretation of the map from other source.

4. Results and discussion

The cover percentages of the result obtained by the best classifier using the January 24, 2001 image were compared with the result found by Woldwahid (2003) using ground surveying. It was found that the risk habitats were larger than the one obtained by ground surveying (Table 4). The sources of the problem for such gap of the two results could be the way of the data collection coupled with the spatial resolution of the sensor. The data used for the present study was collected for the purposes of identifying the desert locust habitats based on ground surveying (section 2.1). MODIS has a spatial resolution of 250 m *250 m, which might overestimate the area.

Table 4. Comparative cover percentage of the risk and non-risk habitats of desert locust by the maximum likelihood classifier using January 24, 2001 image with the cover % obtained by ground surveying (Woldwahid, 2003).

Class	MODIS Image	Ground Surveying
	Area (%)	Area (%)
Risk	14.75	5
No risk	85.25	95

4.6. Prediction of non-surveyed desert locust risk habitats

The spectral signatures of the habitats within the surveyed area were used to check whether prediction could be made for non-surveyed area. Due to cloud cover of the non-surveyed area (Eritrea), it was not possible to get other suitable image during the winter season for the analysis. In addition, there was time limitation to order images of other years and other non-surveyed area. Therefore, MODIS image of November 14, 2000 was used. It was tested in Eritrea between Shirumkelib (17⁰42'N/38⁰23'E) and Akbanazouf Plains (15⁰57N/39⁰12'E). These sites are the focal points of FAO for forecasting desert locust situation (URL 6).

The following map shows the risk habitats of the desert locust (fig 12). As the result shows, risk habits of the desert locust are found near to those sites targeted by FAO and some other parts of the area.

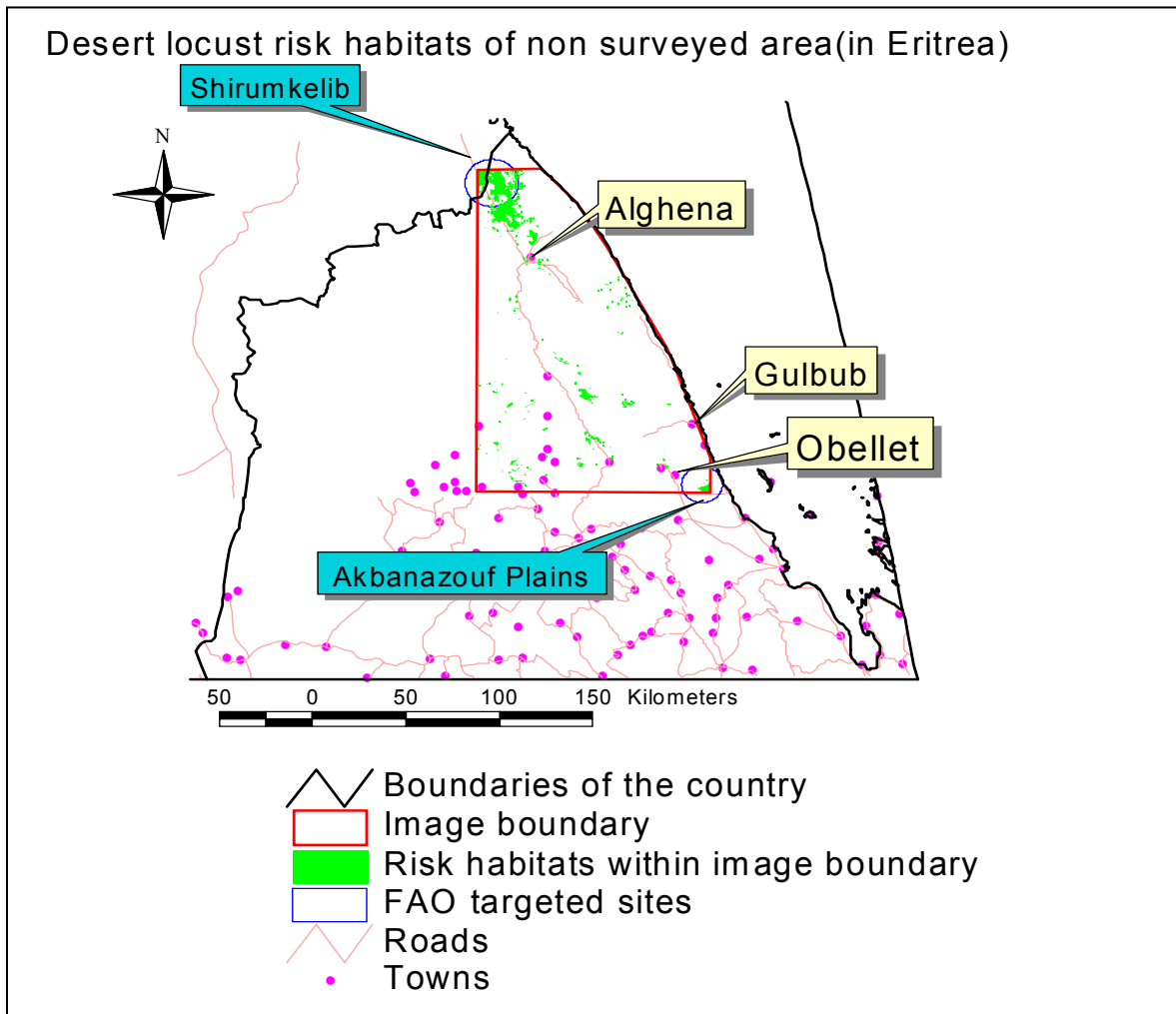


Figure 12. Desert locust habitat of non surveyed areas (Eritrea)

Validation of the result for non surveyed area

The prediction result of non-surveyed area (Eritrea) was sent for validation to experts working at FAO. Dr Keith Cressman, one of the experts, responds

“I would be extremely caution about extrapolating results from Woldewahid's work for several reasons. MODIS imagery evaluated during dry years may under classify or in wet years, it could tend to over classify important DL habitats on the northern Red Sea coast in Eritrea. Even if analysis using a 14.11.2000 MODIS image is a good start, but surely not indicative of potential DL habitat. This year may or may not have been an average year in terms of rainfall. Furthermore, November is at the beginning of the rainy season on the coast. In reality, the majority of the coastal plains from the Akbanazouf Plains to the Sudanese border are very important DL habitat, given sufficient rainfall. Subsequent months should be evaluated and, I would suggest, subsequent years.”

The suggested reason about the date on which the image was taken is right. That is why it was possible to get such image for the analysis. Although the plant community was not there during the analysis period, it is possible to get an overview of the soil type that can support the plant community.

In addition, literature has been searched to check if the risk habitats (Heliotopium plant community) can be found in the coastal plain of Eritrea. It was confirmed that this plant community is common near to Wadies of the Eritrea coastal plan (URL 8).

4.8. Critical reflection

The present study was conducted to explore the possibility of using remote sensing images to give information on the habitats of desert locust, as observed in ground surveys on the Sudanese Red Sea Coast. Such application of linking ground surveying findings to its winter season of satellite image for this area was the first time. Accuracy based classification of habitats and extrapolating the result to non-surveyed habitat to check the possibility of using prediction of the desert locust habitats was the other test of the study. Selecting the best operational sensors for

4. Results and discussion

capturing image in the winter season of the study area was the first task. The next question was looking the possibility of detecting the habitats using image acquired by the best sensor with above 70 % accuracy. This accuracy was selected since it is an acceptable value in remote sensing application depending on the sensors used.

MODIS sensor was found to capture the images with spatial resolution of 250*250 m but high temporal value among the four visited sensors during the winter seasons. A classification accuracy assessment result of the risk habitats of the desert locust using images taken by this sensor with low resolution showed erratic result. For instance, 77.78% user accuracy was obtained using image taken on January 24, 2001. The remaining used images for the analysis did not support such accuracy and resulted in below 70 % user's accuracy. One of the critical reasons for such gap of accuracy could be that the plant cover percentage at this particular season was highest. The ground truth data was also collected near to the image taken (15 the January). This is explained in detail under section 4.2.2. The cover percentage of risk habitat (14 %) obtained by this research is promising provided that there is a gap obtained by ground surveying (5%). Such results were obtained by a sensor, which is freely available, and have a low spatial resolution. In addition, only the spectral information of the plant communities was used for the analysis. Therefore, fieldwork that could agree with the existing resolution of MODIS image as well as including additional information (soil type of the area) for analysis is necessary.

The numbers of the available testing site for the study were not enough to make a valuable accuracy assessment of the classified result (Lillsand and kiefer, 2000). With this, one additional testing site was generated in each of the testing sample sites (section 2.1). This may have an impact on having a best measure of accuracy.

5. Conclusions and Recommendations

5.1. Conclusions

This study investigated the possibility of using remote sensing images for detecting the desert locust on the Sudan Red Sea Coast during the winter season.

Research Question: *Which remote sensing sensor can be used to detect habitats of the desert locust in the Sudan Red Sea Coast during the winter season?*

The results of this study showed that MODIS sensor is the most suitable among the four checked sensors in providing images during the winter season. The most important factor that limited other sensors not to take suitable images was found to be associated with cloudiness of the area as it was rainy season.

Research Question: *Can image of the best sensor be used to identify the desert locust habitat with above 70 % accuracy?*

The detection of desert locust risk habitats was possible with 77.78 % of users accuracy by only using the spectral information of 250 m MODIS images. The result revealed the importance of image acquisition at the right moment or during high cover percentage of the risk habitats.

Research Question: *Which classification algorithms give the best result of identifying the desert locust habitat?*

Maximum likelihood classifier showed the best regardless of the erratic accuracy result. This has been observed depending on the input remote sensing data used for the analysis. Cloud cover of the area reduces the classification accuracy of the desert risk locust habitats. This was observed on the image taken on January 20 and 24, 2001.

Research Question: *Does a multi temporal approach give better accuracy than mono temporal one?*

In this study, mono-temporal approach showed better accuracy than multi-temporal approach in detecting the habitats of the desert locust. But this depends on the probability of getting a cloud free image coupled with high cover percentages of the risk habitats.

Research Question: *Is it possible to make predictions of habitats for desert locust in a non-surveyed area?*

It was possible to predict by extrapolating signatures of the surveyed risk habitat to non-surveyed area (Eritrea). It showed a good start on locating the risk habitats to non-surveyed area.

The methods developed in this study can contribute for mapping the risk habitats of the desert locusts on the basis of MODIS satellite images.

5.2. Recommendations

Only the spectral information of the plant communities from MODIS image was used for the analysis. Using additional information like soil type of the study area can maximize the classification accuracy of detecting habitats of the desert locust on the SRSC.

As this study was the beginning on exploring the potential of using satellite images on the study area, attentions were given to the winter season, which are the growing season of the habitats of the desert locust. As far as the multi temporal analysis is concerned, the probability of getting many suitable images taken during high greenness percentage was very low. MODIS image taken during the summer season was not covered in this study due to time limitation. Therefore, it is advisable to check during summer season in order to have more suitable images (information) and explore the potentials of multi-temporal analysis in improving the classification accuracy. In such way information about the soil condition of the study area as indicator of the possible vegetation type that we will come later can be collected

5. Conclusions and Recommendations

The success of a classification depends not only on the land cover and remotely sensed data type, but also on reference (testing) data. Therefore, it is recommended to have reference data that can agree with the spatial resolution of the MODIS image used for this study.

Due to time limitation predication ability of the developed methods has not been checked with many remote sensing data of the non-surveyed area. Therefore it is recommended to check the developed method using more suitable images of a non-surveyed area and if possible with ground truth.

References

- Cherlet, M., Mathoux, P., Bartholomé, E., & Defourny P., 2000. SPOT VEGETATION Contribution to Desert Locust Habitat Monitoring. In: vegetation 2000 proceedings, 3.-6- April 2000, Space Application Institute, JRC, Ispra, S. 247-257
- Cressman., K., 1996. Monitoring desert locusts in the Middle East: An overview. Yale F & Es Bulletin 103: 125-140.
- FAO, 1977. Application of Landsat data in desert locust survey and control.
- FAO, 1994. The Desert Locust Guidelines: Vol. II. Surver.-, Rome.
- FAO, 1999. Report on the Desert Locust Control Committee (DLCC).
- FAO/USAID, 1980. Remote sensing techniques and methodologies for monitoring ecological conditions for desert locust population development.
- Hardeweg, B and Waibel, H., 2000. New approaches in the assessment of desert locust management in Africa. Hannover, Germany.
- Hielkema, J.U., 1977. Application of Landsat data in desert locust survey and control. Desert locust satellite applications project satage II FAO, Rome.
- Hielkema, J.U., 1980. Remote Sensing techniques and Methodologies for monitoring ecological conditions for desert locust population development. Final technical report., FAO Rome, September 1980.
- Janssen L.L.F, and Gorte B.G.H, 2001. Principle of Remote Sensing, chapter 12 Digital image Classification, International Institute for Aerospace survey and Earth Science, ITC, Enschede, The Netherlands, second edition.
- Jensen, J.R., 1996, Introductory Digital Image Processing, 2nd Ed., Upper Saddle River, NJ: Prentice Hall, 318 pages.
- Johnston, H. B., 1926. A further contribution to our knowledge of bionomics and control of migratory locust, *Schistocerca gregaria* Forsk. (peregrina oliv.), in the Sudan. Wellcome Tropical Research Laboaratory Entomology Section Bulletin 22:14pp.
- Keuchel, J., Naumann, S., Heiler, M., and Siegmund, A., 2003. Automatic land cover analysis for Tenerife by supervised classification using remotely sensing data.
- Krall, S., 1995. Desert locust in Africa--- A Disaster? Disasters 19:1-7.
- Lillesand, T.M., and Kiefer, R.W., 2000. Remote Sensing and Image interpretation. 4th ed. John Wiley and sons, USA.
- Liu, X., 2001. Mapping and Modelling the Habitats of Giant Pandas in Foping Nature Reserve, China ITC Desertation No. 84, ITC, the Netherland. 155 pp.

References

Magor, J.I., and Pender, J., 1997. Desert locust forecasts' GIS: a researchers' view. In: S Krall, R peveling &D Ba Diallo (eds), *New strategies in desert locust control.*: 21-35.

Molenaar, M., 1994. Remote sensing and geographical information processing.

Pax-Lenney, M., C. E. Woodcock, S. A. Maacomber, Gopal, S., and Song, C. 2001. "Forest Mapping with a generalized classifier and Landsat TM data." Remote Sensing of Environment 77(3): 241-250.

PaxLenney, M., & Woodcock, C. E., 1997. Monitoring Agricultural lands in Egypt with Multitemporal Landsat TM Imagery: How Many Images Are Needed? Remote Sensing of Environment, 59, 522- 529.

Pedroni, L., 2003. "Improved classification of Landsat Thematic Mapper data using modified prior probabilities in large and complex landscapes." Remote Sensing 24:91-113.

Piesjio, P., 1992. GIS and Remote Sensing for Soil Erosion Studies in Semi-Arid Environments.

Riley, J.R., and Reynolds, D.R., 1997. Vertical-looking radar as a means to improve forecasting and control of desert locusts. In: S Krall, R peveling &D Ba Diallo (eds), *New strategies in desert locust control.* p. 47-53.

Rogan, D., Cohen, W.B., Berterretche, M., Maiersperger, T.K., and Kennedy, R. E., 2001. "Land cover mapping in an agricultural setting using multi seasonal Thematic Mapper data" Remote Sensing of Environment 76(2): 139-155

Showler, A., 1995. Desert locust control, public health, and environmental sustainability in North Africa, PP. 217-239. In W.D. Swearingen and A. Bencherifa (eds.), *The North African environment at risk.* Westview press, Boulder, CO.

Skaf, R., Popov, G.B., and Roffey, J., 1990. The desert locust: an international challenge. In: *Philosophical transactions of the royal society of London.* 1990, 328:1251,525-538; Paper presented at the discussion "migran pests: problems, potentialities and progress", FAO, Rome.

Steedman, A., 1988. *Locust Handbook.* Overseas Development Agency/National Resources Institute, London, UK.

Tappan, G. G., Moor, G. D., et al., 1991. "Monitoring grasshopper and locust habitats in sahelian Africa using GIS and remote sensing technology." Geographical Information Systems 5(1): 123-135.

Tucker, C.J., Hielkema, J. and Roffey, J., 1995. "The potential of satellite remote sensing of ecological conditions for survey and forecasting Desert locust activity." Remote Sensing 6: 127-138.

Voss, F., and Dreiser, U., 1997. Mapping of desert locust habitats using remote sensing techniques. In: S Krall, R peveling &D Ba Diallo (eds), *New strategies in desert locust control.* p. 37-44.

References

Wagner, D. G., Hoffer, R. M., & Hanson, J. D., 1993. Comparison of multitemporal and unitemporal classification accuracy using Landsat TM imagery. In Looking to the Future with an Eye on the Past (A. J. Lewis, Ed.), ACSM/ASPRS Convention, New Orleans, LA.

Wallin, D., C.H. Elliott, H.H. Shugart, C.J. Tucker., and Wilhelmi, F., 1992. "Satellite remote sensing of breeding habitat for an African weaver-bird." *Landscape Ecology*. 7(2): 87-99

Woldewahid, G. 2003. Habitats and spatial pattern of solitarious desert locust (*Schistocerca gregaria* Forsk.) on the costal plain of Sudan. Ph.D. thesis Wageningen University.

Zhan, Q., 2003. A hierarchical object-based approach for urban land-use classification from remote sensing data. Enschede; Wageningen: ITC; Wageningen University, 2003. PhD thesis Wageningen University; Summaries in Dutch and English (ITC Dissertation; 103)

Websites

URL 1: <http://www.yorku.ca/eye/spectrum.gif>.
Accessed, February 2004.

URL 2: <http://www.fao.org/NEWS/GLOBAL/LOCUSTS/Rsense.htm>.
Accessed, October 2003

URL 3: <http://glervis.usgs.gov/ImgViewer/ImgViewer.html?lat=20.3&lon=36.9&sensor=TM>.
Accessed, July 2003

URL 4: http://www.spotimage.fr/html/_167_171_.php.
Accessed, March 2004

URL 5: <http://edcimswww.cr.usgs.gov/pub/imswelcome/>.
Accessed, September 2003

URL 6: <http://www.cidi.org/locust/DL280e.html>.
Accessed, March 2004

URL 7: <http://www.profc.udec.cl/~gabriel/tutoriales/giswb/vol2/cp5/cp5-8.htm>.
Accessed, April 2004.

URL 8: <http://www.fao.org/DOCREP/004/AB393E/ab393e03.htm>
Accessed, March 2004.

Appendixes

Appendix A. The Error Matrix

		Reference Data				
		Class 1	Class 2	...	Class N	Row total
Classifica- tion Data	Class1	a_{11}	a_{12}		a_{1n}	$\sum_{K=1}^N a_{1K}$
	Class2	a_{21}	a_{22}		a_{2n}	$\sum_{K=1}^N a_{2K}$

	Class N	a_{n1}	a_{n2}		a_{nn}	$\sum_{K=1}^N a_{NK}$
	Column total	$\sum_{K=1}^N a_{K1}$	$\sum_{K=1}^N a_{K2}$		$\sum_{K=1}^N a_{KN}$	$N = \sum_{I,K=1}^N a_{ik}$

Appendix B. MODIS Technical Specifications

Orbit:	705 km, 10:30 a.m. descending node (Terra) or 1:30 p.m. ascending node (Aqua), sun-synchronous, near-polar, circular
Scan Rate:	20.3 rpm, cross track
Swath Dimensions:	2330 km (cross track) by 10 km (along track at nadir)
Telescope:	17.78 cm diam. off-axis, afocal (collimated), with intermediate field stop
Size:	1.0 x 1.6 x 1.0 m
Weight:	228.7 kg
Power:	162.5 W (single orbit average)
Data Rate:	10.6 Mbps (peak daytime); 6.1 Mbps (orbital average)
Quantization:	12 bits
Spatial Resolution:	250 m (bands 1-2) 500 m (bands 3-7) 1000 m (bands 8-36)
Design Life:	6 years

Appendixes

Primary Use	Band	Bandwidth ¹	Spectral Radiance ²	Required SNR ³
Land/Cloud/Aerosols Boundaries	1	620 - 670	21.8	128
	2	841 - 876	24.7	201
Land/Cloud/Aerosols Properties	3	459 - 479	35.3	243
	4	545 - 565	29.0	228
	5	1230 - 1250	5.4	74
	6	1628 - 1652	7.3	275
	7	2105 - 2155	1.0	110
Ocean Color/ Phytoplankton/ Biogeochemistry	8	405 - 420	44.9	880
	9	438 - 448	41.9	838
	10	483 - 493	32.1	802
	11	526 - 536	27.9	754
	12	546 - 556	21.0	750
	13	662 - 672	9.5	910
	14	673 - 683	8.7	1087
	15	743 - 753	10.2	586
	16	862 - 877	6.2	516
Atmospheric Water Vapor	17	890 - 920	10.0	167
	18	931 - 941	3.6	57
	19	915 - 965	15.0	250

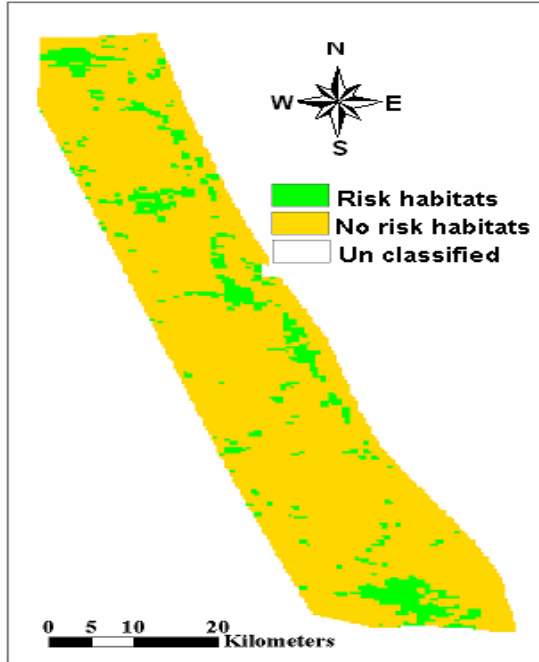
Primary Use	Band	Bandwidth ¹	Spectral Radiance ²	Required NE[delta]T(K) ⁴
Surface/Cloud Temperature	20	3.660 - 3.840	0.45(300K)	0.05
	21	3.929 - 3.989	2.38(335K)	2.00
	22	3.929 - 3.989	0.67(300K)	0.07
	23	4.020 - 4.080	0.79(300K)	0.07
Atmospheric Temperature	24	4.433 - 4.498	0.17(250K)	0.25
	25	4.482 - 4.549	0.59(275K)	0.25
Cirrus Clouds Water Vapor	26	1.360 - 1.390	6.00	150(SNR)
	27	6.535 - 6.895	1.16(240K)	0.25
	28	7.175 - 7.475	2.18(250K)	0.25
Cloud Properties	29	8.400 - 8.700	9.58(300K)	0.05
Ozone	30	9.580 - 9.880	3.69(250K)	0.25
Surface/Cloud Temperature	31	10.780 - 11.280	9.55(300K)	0.05
	32	11.770 - 12.270	8.94(300K)	0.05
Cloud Top Altitude	33	13.185 - 13.485	4.52(260K)	0.25
	34	13.485 - 13.785	3.76(250K)	0.25
	35	13.785 - 14.085	3.11(240K)	0.25
	36	14.085 - 14.385	2.08(220K)	0.35

¹ Bands 1 to 19 are in nm; Bands 20 to 36 are in μm
² Spectral Radiance values are ($\text{W}/\text{m}^2 \cdot \mu\text{m}\cdot\text{sr}$)
³ SNR = Signal-to-noise ratio
⁴ NE(δ)T = Noise-equivalent temperature difference
Note: Performance goal is 30-40% better than required

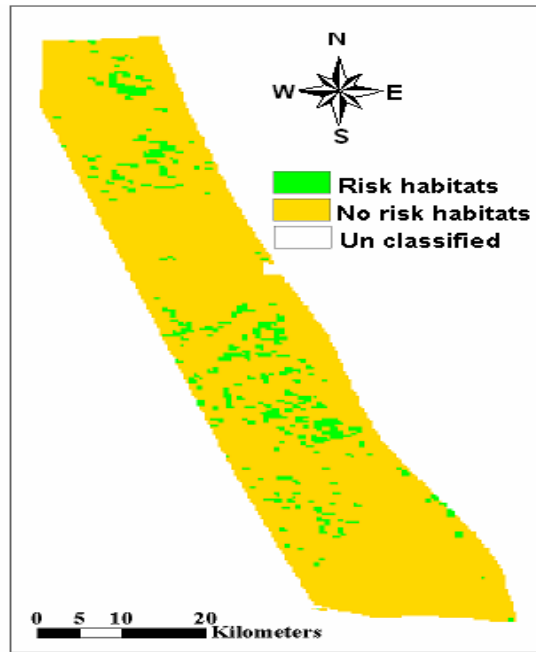
Appendix C: Classification result of mono-temporal image

Figure1. Desert locust habitats using the four classifiers: November 14, 2000 image.

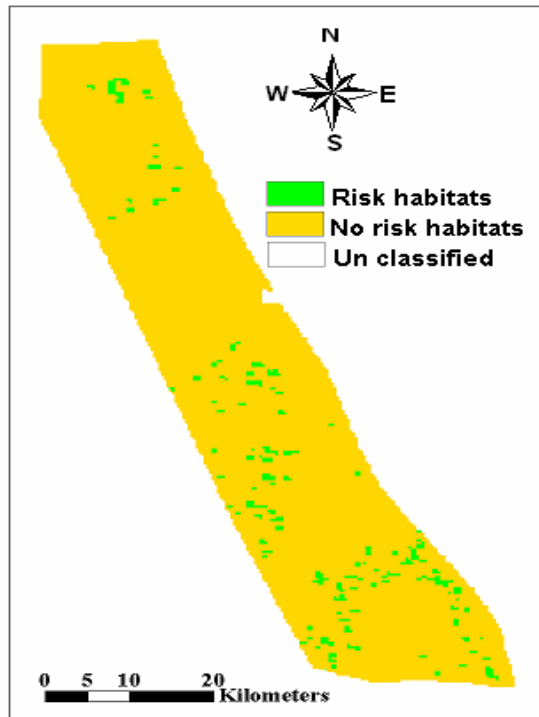
a. Maximum likelihood classifier



b. Minimum distance to means classifier



c. Mahalanobis classifier



d. Parallelepiped classifier

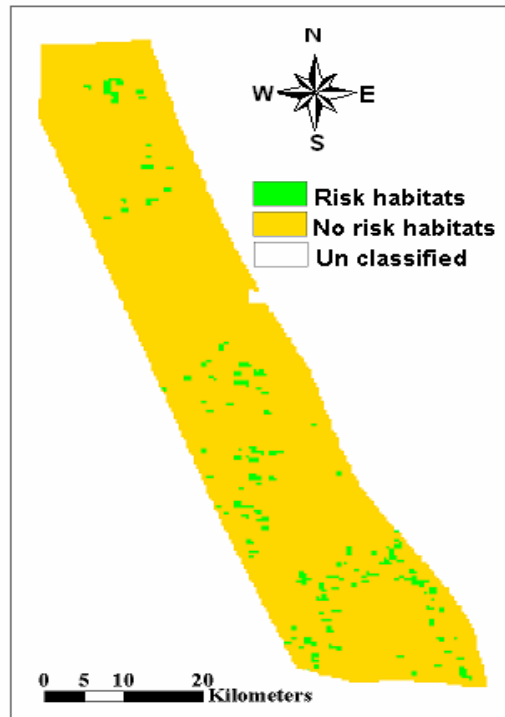
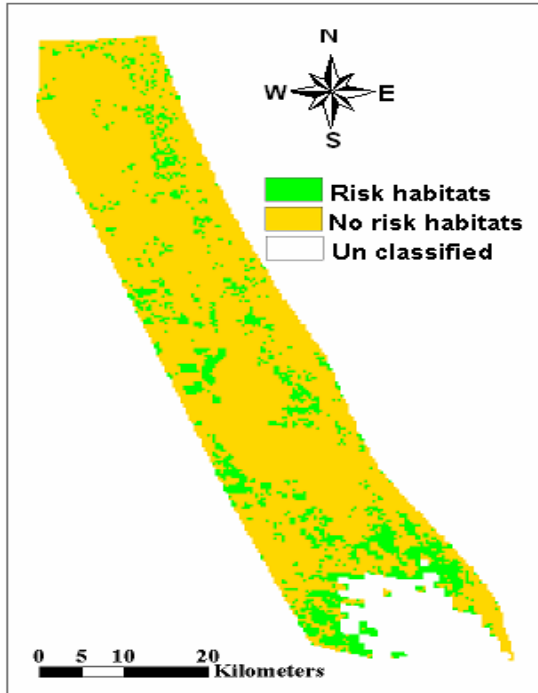
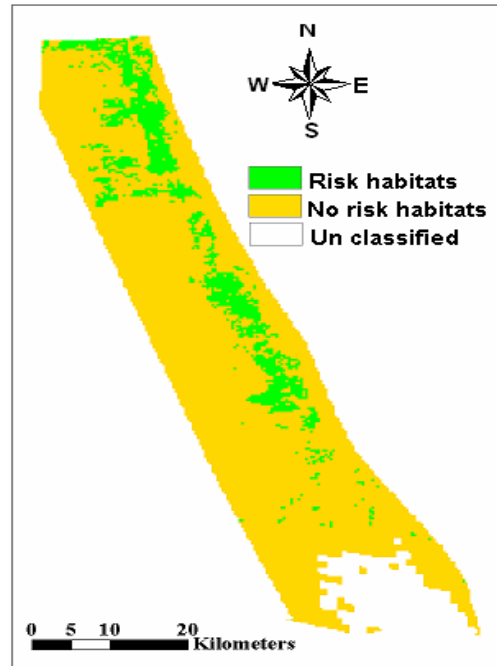


Figure2. Desert locust habitats using the four classifier: Januar20, 2001 image.

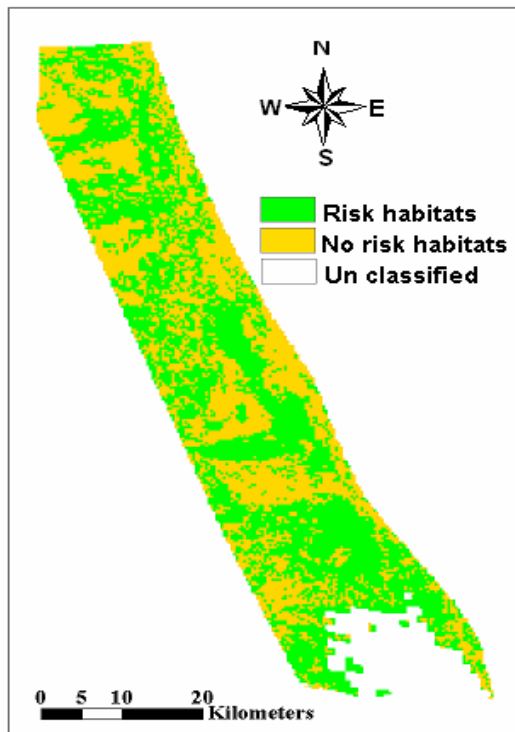
a. Maximum likelihood classifier



b. Minimum distance to means classifier



c. Mahalanobis classifier



Parallelepiped classifier

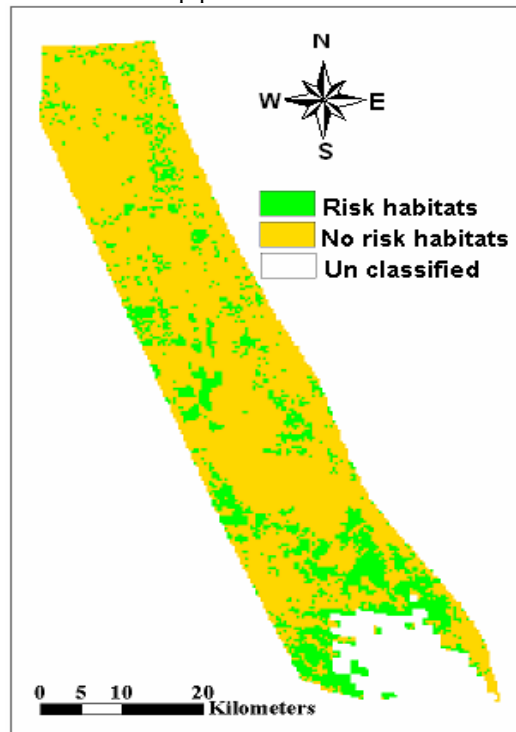
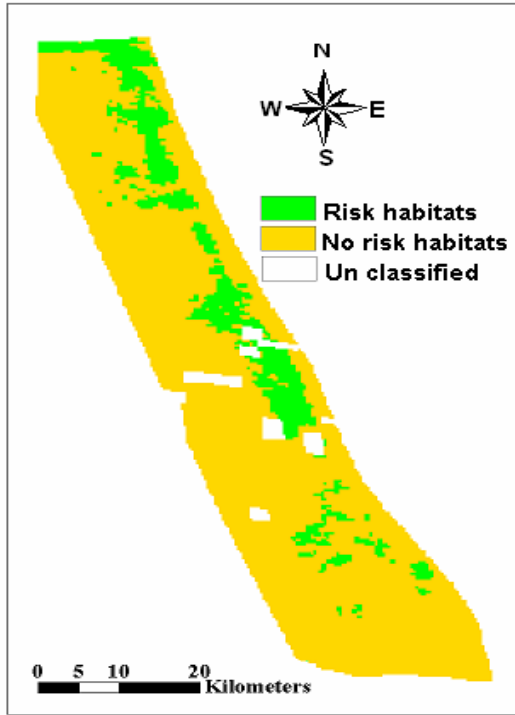
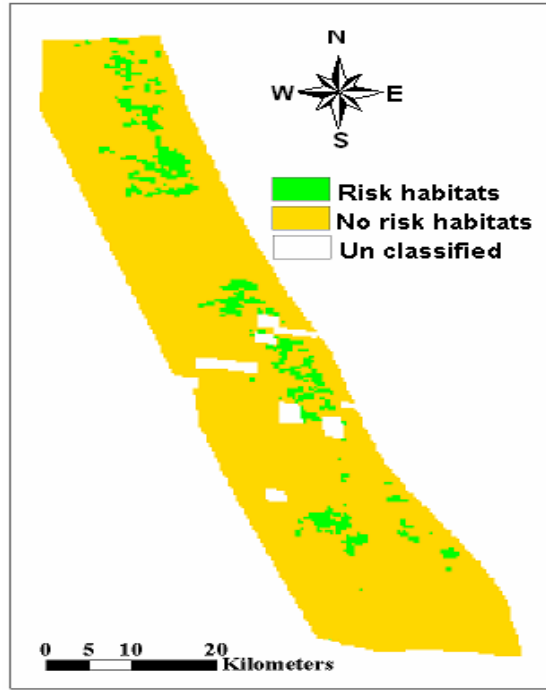


Figure3. Desert locust habitats using the four classifiers: Januar24, 2000 image.

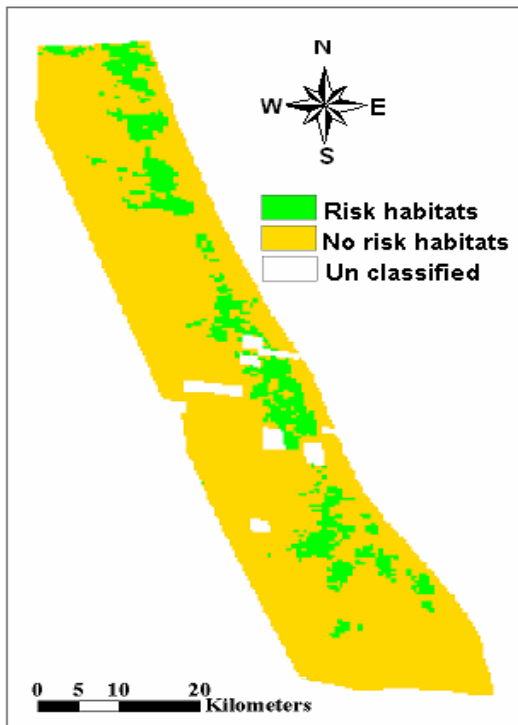
a. Maximum likelihood classifier



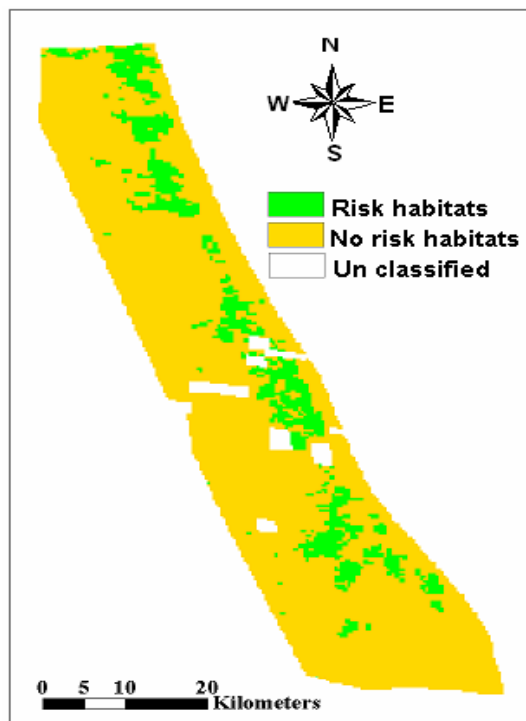
b. Minimum distance to means classifier



c. Mahalanobis classifier



d. Parallelepiped classifier



Appendix D. Accuracy assessments of mono-temporal images

Table 1. Accuracy assessment results of the four classifiers using November 14, 2000 image

a. Maximum likelihood classifier

Classified data	Unclassified	Reference data		Row total	Producer's accuracy (%)	User's accuracy (%)	Overall accuracy (%)
		Risk	No risk				
Unclassified	0	0	0	0			
Risk	0	5	5	10	22.73	50.00	73.17
No risk	0	17	55	72	91.67	76.39	
Column Total	0	22	60	82			

b. Minimum distance to means classifier

Classified data	Unclassified	Reference data		Row total	Producer's accuracy (%)	User's accuracy (%)	Overall accuracy (%)
		Risk	No risk				
Unclassified	0	0	0	0			
Risk	0	2	12	14	9.09	14.29	60.98
No risk	0	20	48	68	80.00	70.59	
Column Total	0	22	60	82			

c. Mahalanobis classifier

Classified data	Unclassified	Reference data		Row total	Producer's accuracy (%)	User's accuracy (%)	Overall accuracy (%)
		Risk	No risk				
Unclassified		0	0	0			
Risk		0	2	2	0.00	0.00	70.73
No risk		22	58	80	96.67	72.50	
Column Total		22	60	82			

d. Parallelepiped classifier

Classified data	Unclassified	Reference data		Row total	Producer's accuracy (%)	User's accuracy (%)	Overall accuracy (%)
		Risk	No risk				
Unclassified	0	0	0	0			
Risk	0	3	16	19	0.00	0.00	70.73
No risk	0	18	43	61	96.67	72.50	
Column Total	0	22	60	82			

Table2. Accuracy assessment results of the four classifiers using January 20, 2001 image

a. Maximum likelihood classifier

Classified data	Unclassified	Reference data		Row total	Producer's accuracy (%)	Users' accuracy (%)	Overall accuracy (%)
		Risk	No risk				
Unclassified	0	0	0	0			
Risk	0	5	5	10	29.00	50.00	79.00
No risk	0	12	48	60	91.00	80.00	
Column Total	0	17	53	70			

b. Minimum distance to means classifier

Classified data	Unclassified	Reference data		Row total	Producer accuracy (%)	Users' accuracy (%)	Overall accuracy (%)
		Risk	No risk				
Unclassified	0	0	0	0			
Risk	0	9	5	14	52.94	64.29	81.43
No risk	0	8	48	56	90.57	85.71	
Column Total	0	17	53	70			

c. Mahalanobis classifier

Classified data	Unclassified	Reference data		Row total	Producer accuracy (%)	Users' accuracy (%)	Overall accuracy (%)
		Risk	No risk				
Unclassified	0	0	0	0			
Risk	0	7	34	41	41	17	37
No risk	0	10	19	29	36	66	
Column Total	0	17	53	70			

d. Parallelepiped classifier

Classified data	Unclassified	Reference data		Row total	Producer accuracy (%)	Users' accuracy (%)	Overall accuracy (%)
		Risk	No risk				
Unclassified	0	0	0	0			
Risk	0	5	9	14	29	36	77
No risk	0	12	44	56	98	93	
Column Total	0	17	53	70			

Table3. Accuracy assessment results of the four classifiers using January 24, 2001 image:

a. Maximum likelihood classifier

Classified data	Unclassified	Reference data			Producer accuracy (%)	Users' accuracy (%)	Overall accuracy (%)
		Risk	No risk	Row total			
Unclassified	0	0	1	1			
Risk	0	14	4	18	70.00	77.78	86.25
No risk	0	6	55	61	91.67	90.16	
Column Total	0	20	60	80			

b. Minimum distance to means classifier

Classified data	Unclassified	Reference data			Producer accuracy (%)	Users' accuracy (%)	Overall accuracy (%)
		Risk	No risk	Row total			
Unclassified	0	0	1	1			
Risk	0	2	4	6	10.00	33.33	72.50
No risk	0	18	55	73	91.67	75.34	
Column Total	0	20	60	80			

c. Mahalanobis classifier

Classified data	Unclassified	Reference data			Producer accuracy (%)	Users accuracy (%)	Overall accuracy (%)
		Risk	No risk	Row total			
Unclassified	0	0	1	1			
Risk	0	11	8	19	55.00	57.89	77.50
No risk	0	9	51	60	85.00	85.00	
Column Total	0	20	60	80			

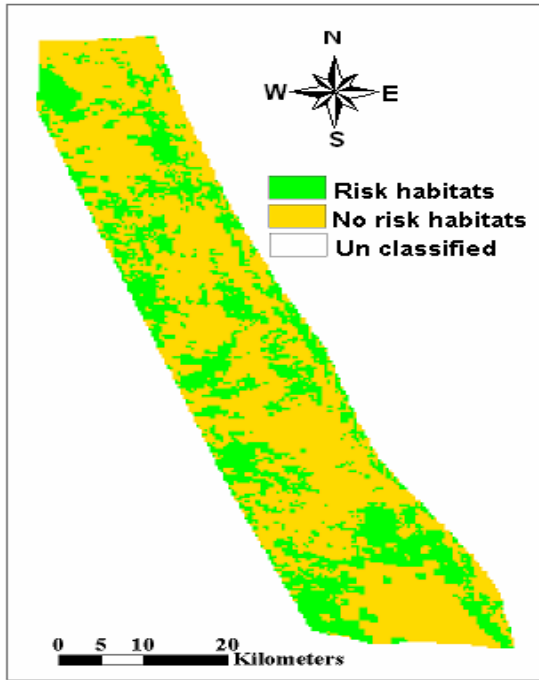
d. Parallelepiped classifier

Classified data	Unclassified	Reference data			Producer's accuracy (%)	User's accuracy (%)	Overall accuracy (%)
		Risk	No risk	Row total			
Unclassified		0	1	1			
Risk		10	8	18	50.00	55.56	76.25
No risk		10	51	61	85.00	83.61	
Column Total		20	60	80			

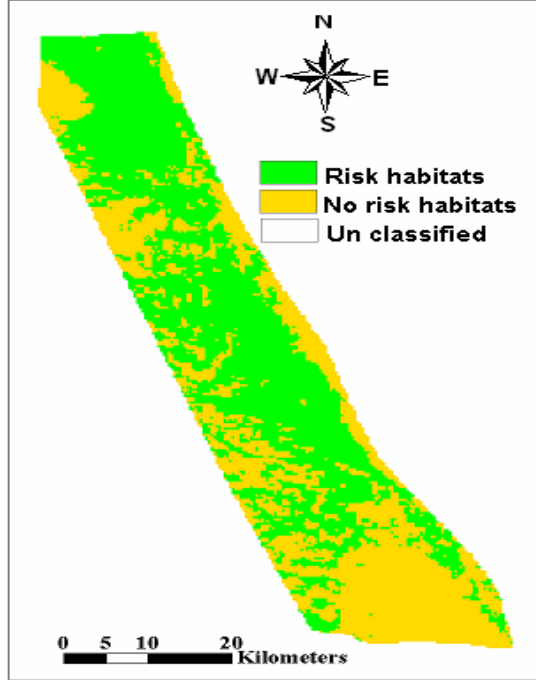
Appendix E: Classification result of multi-temporal images

Figure1. Desert locust habitats using the four classifiers: November 14, 2000, and January 20, 2001 images.

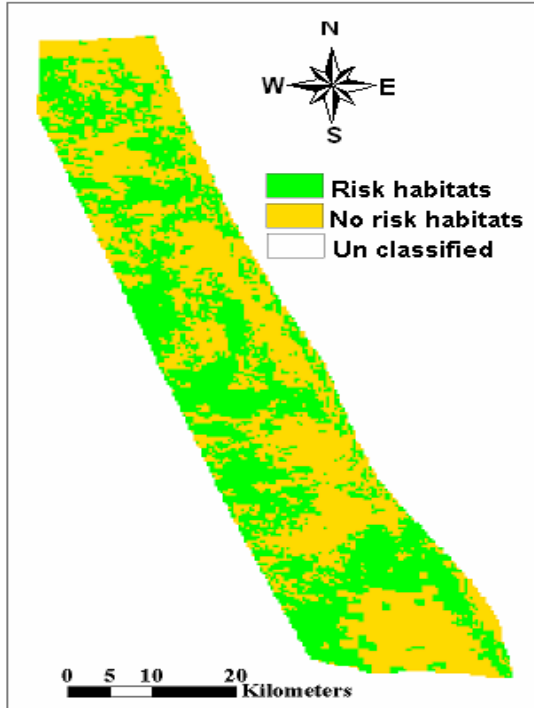
a. Maximum likelihood classifier



b. Minimum distance to means classifier



c. Mahalanobis classifier



d. Parallelepiped classifier

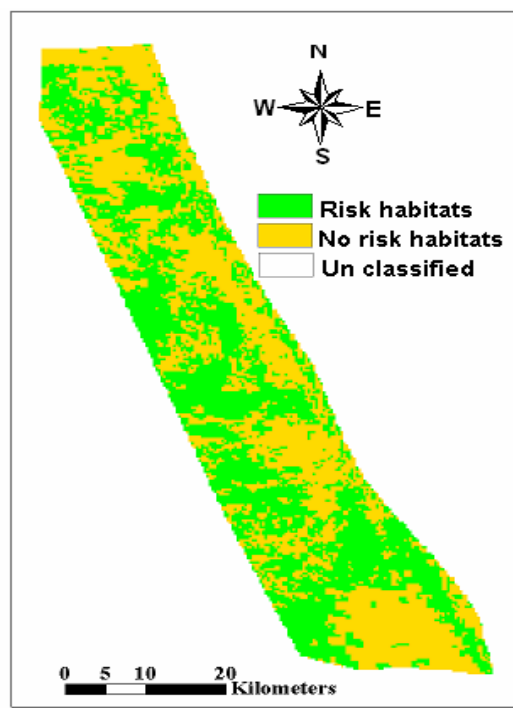
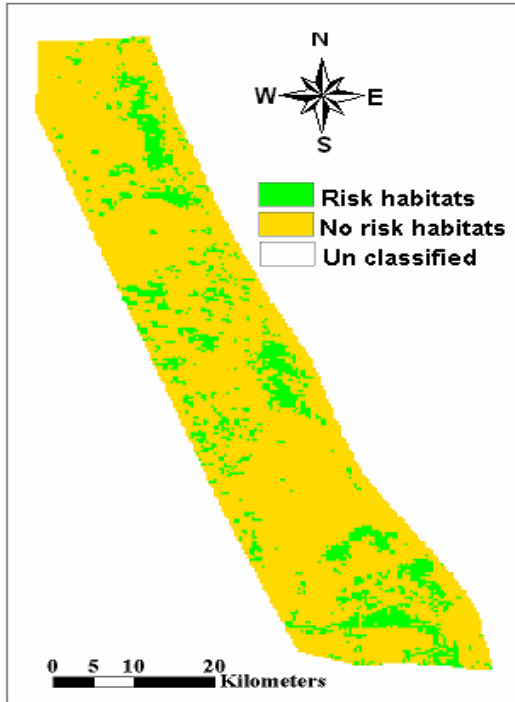
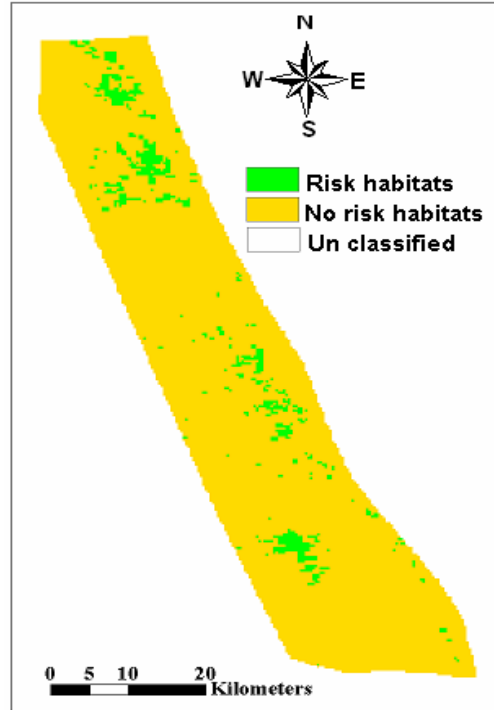


Figure 2. Desert locust habitats using the four classifier: Nov.14, 00 and Jan. 24, 01 image.

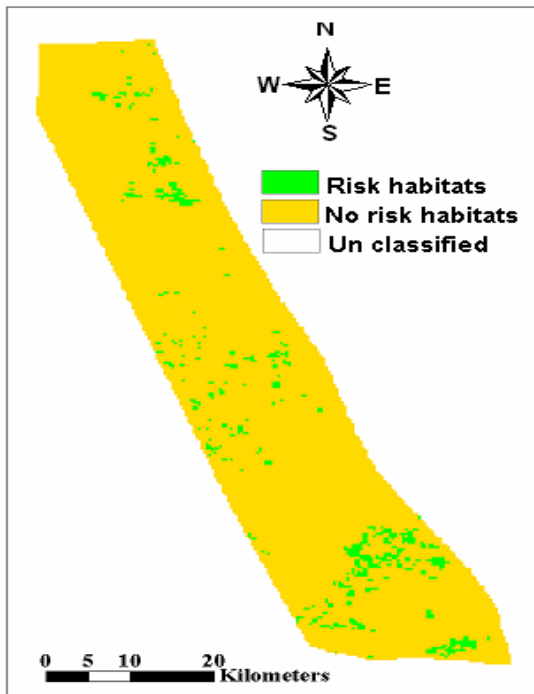
a. Maximum likelihood classifier



b. Minimum distance to means classifier



c. Mahalanobis classifier



Parallelepiped classifier

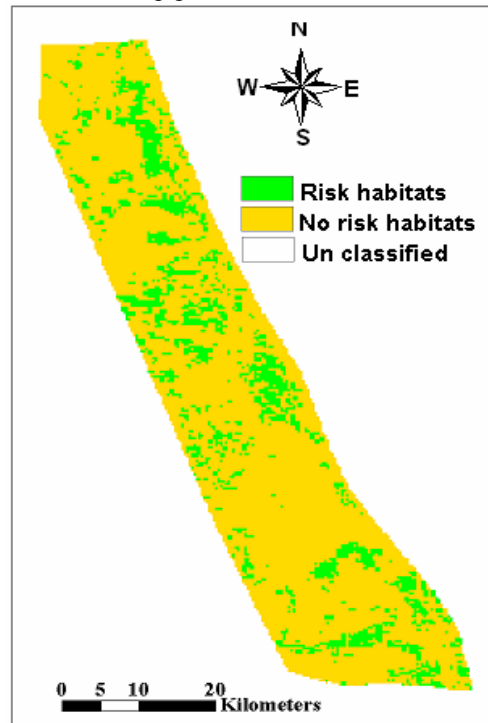
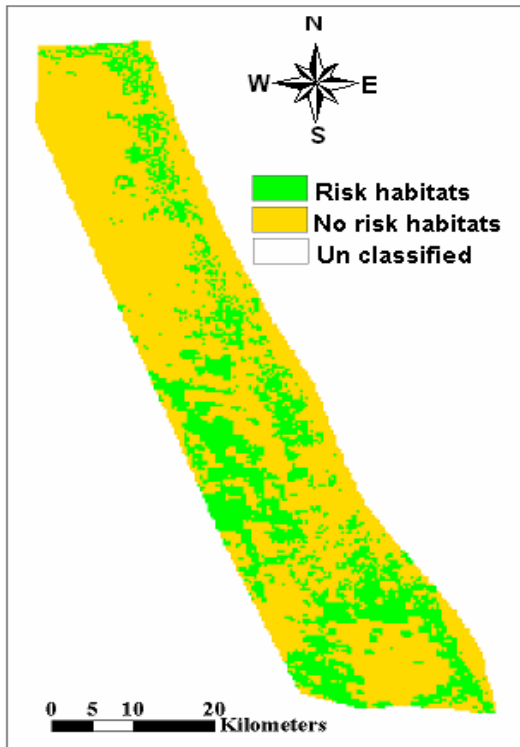
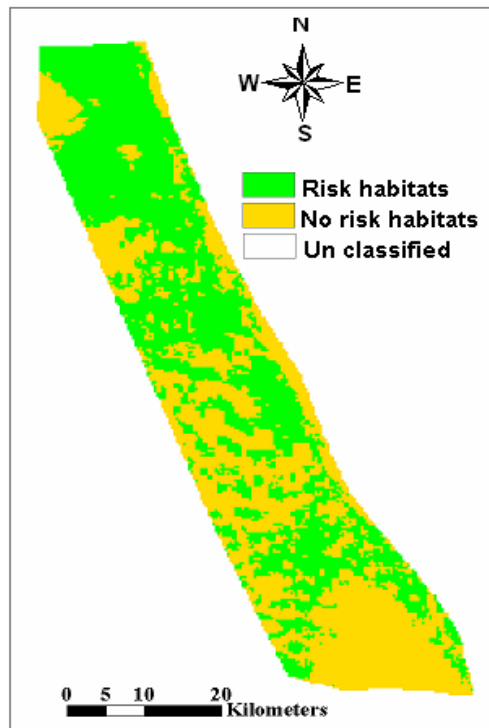


Figure3. Desert locust habitats using the four classifiers: January 20 and 24, 2000 image.

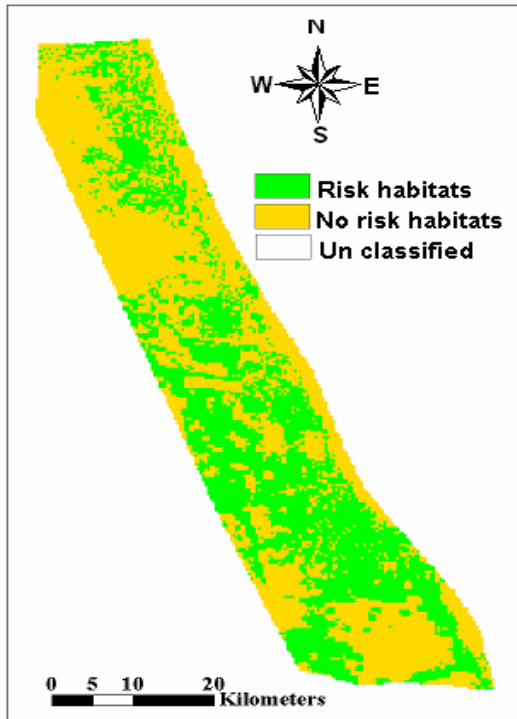
a. Maximum likelihood classifier



b. Minimum distance to means classifier



c. Mahalanobis classifier



d. Parallelepiped classifier

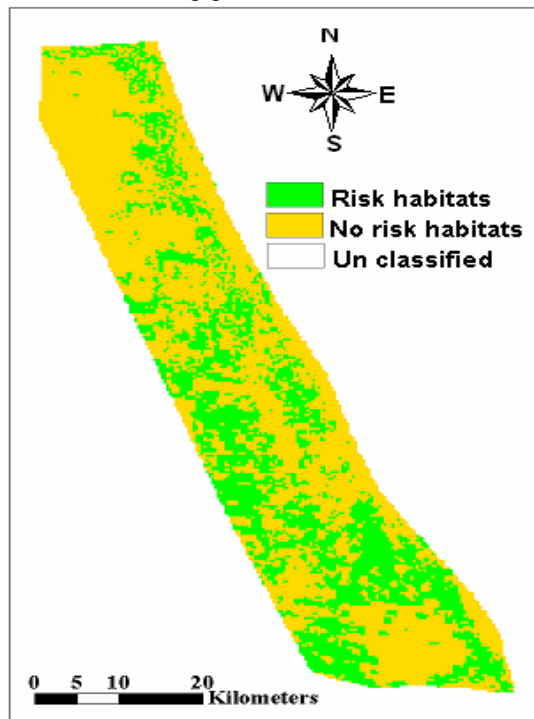
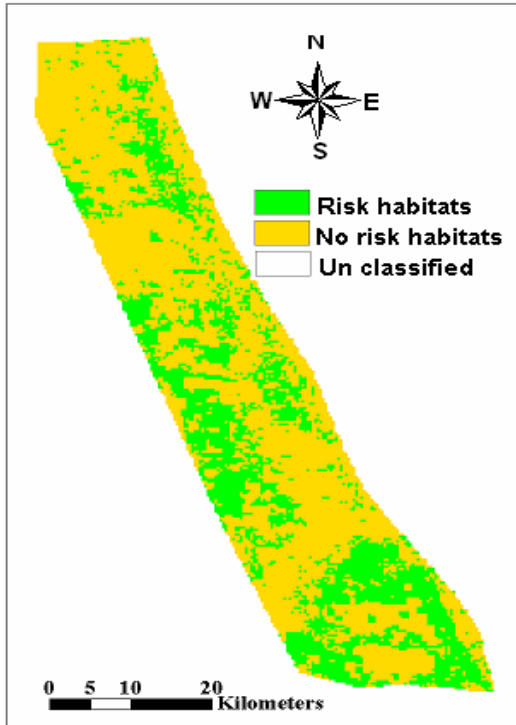
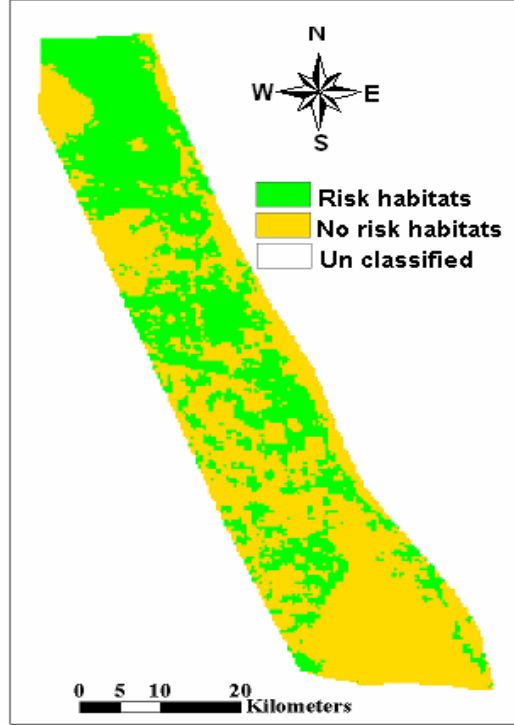


Figure 3. Desert locust habitats using the four classifiers: Nov14, 00, Jan20 and 24, 2001 image.

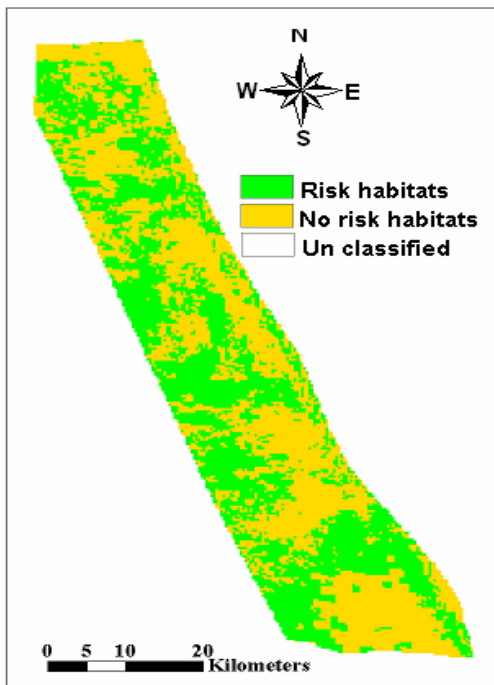
a. Maximum likelihood classifier



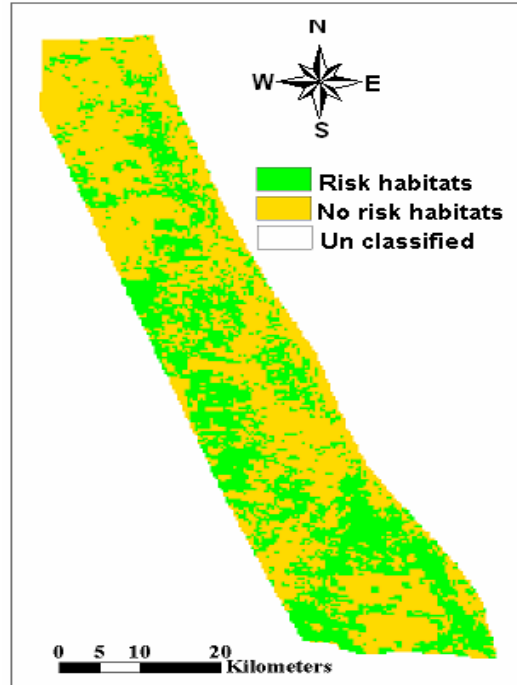
b. Minimum distance to means classifier



c. Mahalanobis classifier



d. Parallelepiped classifier



Appendix F. Accuracy assessments of multi-temporal images

Table 4. Accuracy assessment results of the four classifiers using combined image of November 14, 2000 and January 20, 2001

a. Maximum likelihood classifier

Classified data	Unclassified	Reference data		Row total	Producer's accuracy (%)	User's accuracy (%)	Overall accuracy (%)
		Risk	No risk				
Unclassified	0	0	0	0			
Risk	0	10	17	27	45.45	37.04	64.63
No risk	0	12	43	55	71.67	78.18	
Column Total	0	22	60	82			

b. Minimum distance to means classifier

Classified data	Unclassified	Reference data		Row total	Producer's accuracy (%)	Users accuracy (%)	Overall accuracy (%)
		Risk	No risk				
Unclassified	0	0	0	0			
Risk	0	11	42	53	50.00	20.75	35.37
No risk	0	11	18	29	30.00	62.07	
Column Total	0	22	60	82			

c. Mahalanobis classifier

Classified data	Unclassified	Reference data		Row total	Producer's accuracy (%)	Users accuracy (%)	Overall accuracy (%)
		Risk	No risk				
Unclassified	0	0	0	0			
Risk	0	5	28	33	22.73	15.15	57.32
No risk	0	17	42	59	70.00	85.71	
Column Total	0	22	60	82			

d. Parallelepiped classifier

Classified data	Unclassified	Reference data		Row total	Producer's accuracy (%)	Users accuracy (%)	Overall accuracy (%)
		Risk	No risk				
Unclassified	0	0	0	0			
Risk	0	6	34	40	27.27	15.00	39.02
No risk	0	16	26	42	43.33	61.90	
Column Total	0	22	60	82			

Table 5. Accuracy assessment results of the four classifiers using the combined images of November 14, 2001/January 24, 2001 image

a. Maximum likelihood classifier

Classified data	Unclassified	Reference data			Producers' accuracy (%)	Users' accuracy (%)	Overall accuracy (%)
		Risk	No risk	Row total			
Unclassified	0	0	0	0			
Risk	0	8	8	16	36.36	50.00	73.17
No risk	0	14	52	66	86.67	78.79	
Column Total	0	22	60	82			

b. Minimum distance to means classifier

Classified data	Unclassified	Reference data			Producer accuracy (%)	Users' accuracy (%)	Overall accuracy (%)
		Risk	No risk	Row total			
Unclassified	0	0	0	0			
Risk	0	4	7	11	18.18	36.36	69.51
No risk	0	18	53	71	88.33	74.65	
Column Total	0	22	60	82			

c. Mahalanobis classifier

Classified data	Unclassified	Reference data			Producer accuracy (%)	Users' accuracy (%)	Overall accuracy (%)
		Risk	No risk	Row total			
Unclassified	0	0	0	0			
Risk	0	3	5	8	13.64	37.50	70.73
No risk	0	19	55	74	91.67	74.32	
Column Total	0	22	60	82			

d. Parallelepiped classifier

Classified data	Unclassified	Reference data			Producer accuracy (%)	Users' accuracy (%)	Overall accuracy (%)
		Risk	No risk	Row total			
Unclassified	0	0	0	0			
Risk	0	7	8	15	31.82	46.67	71.95
No risk	0	15	52	67	86.67	77.61	
Column Total	0	17	53	70			

Table6. Accuracy assessment results of the four classifiers using the combine image of January 20, and 24, 2001 images

a. Maximum likelihood classifier

Classified data	Unclassified	Reference data			Producer accuracy (%)	Users' accuracy (%)	Overall accuracy (%)
		Risk	No risk	Row total			
Unclassified	0	0	0	0			
Risk	0	14	15	29	63.64	48.28	71.95
No risk	0	8	45	53	75.00	84.91	
Column Total	0	22	60	82			

b. Minimum distance to means classifier

Classified data	Unclassified	Reference data			Producer accuracy (%)	Users' accuracy (%)	Overall accuracy (%)
		Risk	No risk	Row total			
Unclassified	0	0	0	0			
Risk	0	13	42	55	59.09	23.64	37.80
No risk	0	9	18	27	30.00	66.67	
Column Total	0	22	60	82			

c. Mahalanobis classifier

Classified data	Unclassified	Reference data			Producer accuracy (%)	Users accuracy (%)	Overall accuracy (%)
		Risk	No risk	Row total			
Unclassified	0	0	0	0			
Risk	0	12	35	47	54.55	25.53	45.12
No risk	0	10	25	35	41.67	71.43	
Column Total	0	22	60	82			

d. Parallelepiped classifier

Classified data	Unclassified	Reference data			Producer's accuracy (%)	User's accuracy (%)	Overall accuracy (%)
		Risk	No risk	Row total			
Unclassified	0	0	0	0			
Risk	0	15	25	40	68.18	37.50	60.98
No risk	0	7	35	42	58.33	83.33	
Column Total	0	22	60	82			

Table 7. Accuracy assessment results of the four classifiers using the combine image of November 14, 2000; 20, and 24, 2001 images

a. Maximum likelihood classifier

Classified data	Unclassified	Reference data			Producer accuracy (%)	Users' accuracy (%)	Overall accuracy (%)
		Risk	No risk	Row total			
Unclassified	0	0	0	0			
Risk	0	10	15	25	45.45	40.00	67.07
No risk	0	12	45	57	75.00	78.95	
Column Total	0	22	60	82			

b. Minimum distance to means classifier

Classified data	Unclassified	Reference data			Producer accuracy (%)	Users' accuracy (%)	Overall accuracy (%)
		Risk	No risk	Row total			
Unclassified	0	0	0	0			
Risk	0	9	32	41	40.91	21.95	45.12
No risk	0	13	28	41	46.67	68.29	
Column Total	0	22	60	82			

c. Mahalanobis classifier

Classified data	Unclassified	Reference data			Producer accuracy (%)	Users accuracy (%)	Overall accuracy (%)
		Risk	No risk	Row total			
Unclassified	0	0	0	0			
Risk	0	8	17	25	36.36	32.00	62.20
No risk	0	14	43	57	71.67	75.44	
Column Total	0	22	60	82			

d. Parallelepiped classifier

Classified data	Unclassified	Reference data			Producer's accuracy (%)	User's accuracy (%)	Overall accuracy (%)
		Risk	No risk	Row total			
Unclassified	0	0	0	0			
Risk	0	10	24	34	45.45	29.41	56.10
No risk	0	12	36	48	60.00	75.00	
Column Total	0	22	60	82			

Appendix G. Histogram and feature space plot of Jan 20, 2001 MODIS image

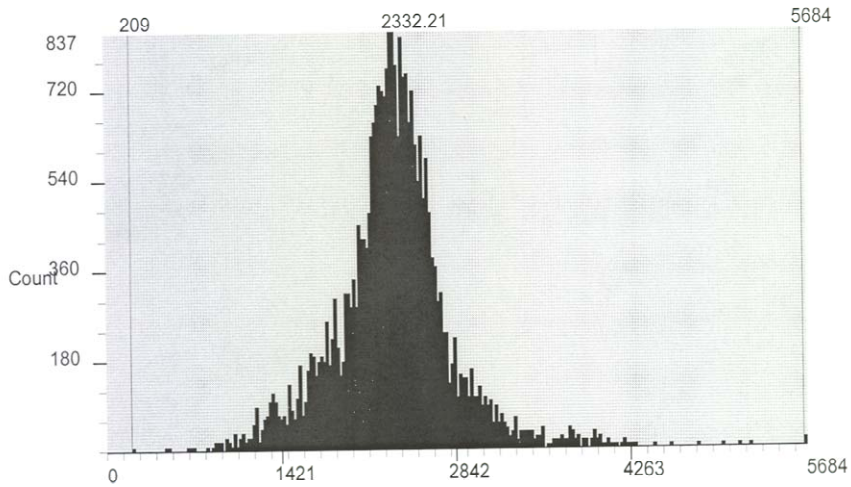


Figure 1. The histogram of pixel values (shows normal distribution)

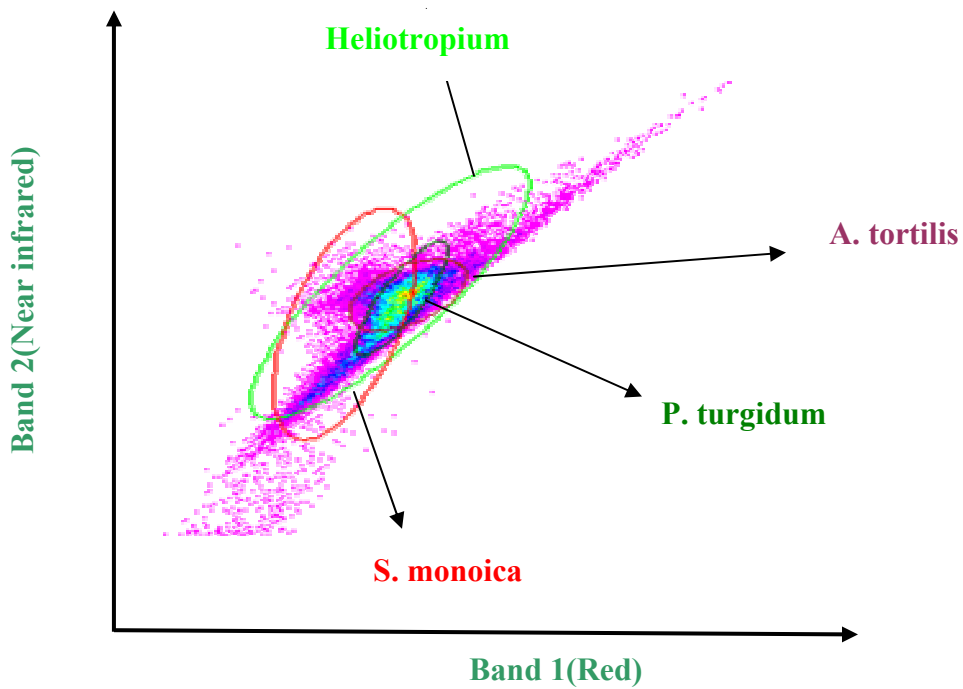


Figure 2. Distributions of the four plant communities in the feature space plot.